

## AN ISOCHRON METHOD FOR COSMOGENIC-NUCLIDE DATING OF BURIED SOILS AND SEDIMENTS

GREG BALCO<sup>\*,\*\*\*,†</sup>, and CHARLES W. ROVEY II<sup>\*\*</sup>

**ABSTRACT.** We describe an improved method for dating buried paleosols using measurements of the cosmic-ray-produced radionuclides  $^{10}\text{Be}$  and  $^{26}\text{Al}$  in quartz grains, and apply it to a sequence of intercalated tills and paleosols in central Missouri, USA, that record Plio-Pleistocene advances of the Laurentide Ice Sheet. A buried paleosol implies a period of surface exposure and nuclide accumulation, followed by burial and a halt to nuclide production. If the paleosol is formed in a sedimentary unit such as till, this unit may also have been emplaced with unknown  $^{26}\text{Al}$  and  $^{10}\text{Be}$  concentrations inherited from past surface exposure. If the inherited nuclide concentrations are the same at all depths in the soil—as is true for well-mixed sediments such as till—then the  $^{26}\text{Al}$  and  $^{10}\text{Be}$  concentrations at different depths in the paleosol will show a linear relationship. The slope of this line depends on the duration of burial of the paleosol, but not on the inherited nuclide concentrations or on the sample depths. Thus, one can date strata overlying buried paleosols by measuring  $^{26}\text{Al}$  and  $^{10}\text{Be}$  at multiple depths in the paleosol and calculating the burial age of the paleosol from the resulting isochron. We focus on applying this approach to till-paleosol sequences, but the basic idea of forming an  $^{26}\text{Al}$ - $^{10}\text{Be}$  burial isochron with a set of samples that share the same burial age, but differ in other aspects of their exposure history, applies to other stratigraphic settings as well. The method yields ages for four tills in Missouri that are stratigraphically consistent, agree with paleomagnetic age constraints, and show that ice advanced into Missouri near 1.25 Ma, near 0.8 Ma, and twice between ca. 0.4 and 0.2 Ma.

### INTRODUCTION

This paper describes a new method of dating buried paleosols and other sediments using the cosmic-ray-produced radionuclides  $^{26}\text{Al}$  and  $^{10}\text{Be}$ , that generalizes existing methods of ‘burial dating’. The basic idea of  $^{26}\text{Al}$ - $^{10}\text{Be}$  burial dating is that these nuclides are produced at a fixed ratio during cosmic-ray bombardment of quartz grains at the Earth’s surface, but have different half-lives. Quartz exposed at the surface for a time has  $^{26}\text{Al}$  and  $^{10}\text{Be}$  concentrations that conform to the production ratio. If it is subsequently buried deeply enough to be shielded from the cosmic-ray flux, the inventories of the two nuclides decay at different rates. Their ratio diverges from the production ratio and can be used as a burial clock. This idea originated with studies of cosmogenic nuclides in meteorites and has since been applied in a variety of terrestrial settings, most commonly to date river sediments buried in caves (see Granger, 2006, for a complete summary of the development and applications of burial dating).

$^{26}\text{Al}$ - $^{10}\text{Be}$  burial dating is, in principle, an attractive technique for dating stratified sediments because it only requires quartz-bearing sediment that has been exposed for a time near the Earth’s surface and then sequestered in a stratigraphic section—neither the presence of fossils or the syndepositional formation of new minerals is needed. As quartz-bearing sediment is ubiquitous in most geologic settings, the technique has the potential to address several important geologic problems that have not yet been solved because of a lack of applicable dating methods. For example, our overall motivation in this project is to develop new methods of dating Plio-Pleistocene

\*Quaternary Research Center and Department of Earth and Space Sciences, University of Washington, Seattle, Washington 98195-1310 USA

\*\*Geography, Geology, and Planning, Missouri State University, Springfield, Missouri 65897 USA

\*\*\*Present address: Berkeley Geochronology Center, 2455 Ridge Road, Berkeley, California 94709 USA

†Corresponding author: balcs@bgc.org

glacial sediments. This is important because present and former continental ice sheets are surrounded by thick sequences of tills and associated ice-marginal sediments, and these stratigraphic sequences are the primary record of ice sheet advances and retreats during the last several million years. Most of what we know about the chronology of Plio-Pleistocene ice advances, however, does not come from this direct stratigraphic evidence, but from oxygen-isotope records in marine sediment cores (Emiliani, 1955; Shackleton and Opdyke, 1973). In general, the marine records record only global ice volume and give little information about the size, location, or even the existence of specific continental ice sheets during particular oxygen isotope excursions. Continental stratigraphic sequences contain this information, but so far they have proven to be extremely difficult to date. In the region formerly occupied by the Laurentide Ice Sheet, for example, the only widely applicable methods for dating glacial sediments older than the useful ranges of radiocarbon ( $\sim 50,000$  yr) or optical dating techniques ( $\sim 150,000$  yr) are by bracketing them between two magnetic reversals or three widespread ashes from the Yellowstone volcanic center. These time markers are separated by hundreds of thousands of years, and only a few stratigraphic sections contain any of them at all. The result is that it is impossible to associate most individual Plio-Pleistocene tills with particular marine oxygen isotope stages, and there exists little direct evidence to show whether or not the configuration of ice sheets during older glaciations was or was not similar to that during the most recent one. This, in turn, is a serious obstacle to understanding the origin and evolution of the glacial-interglacial cycles that are the defining feature of the last several million years of Earth history.

We originally sought to apply the idea of burial dating to early and middle Pleistocene glacial sediments because glacial stratigraphic sections in north-central North America largely consist of tills separated by interglacial paleosols and river sediments. This stratigraphy indicates that the interglacial units were exposed to the surface cosmic-ray flux during their formation, and then buried by till during ice sheet advances. If the overlying till is thick enough to effectively stop the cosmic-ray flux, the cosmogenic-nuclide burial age of the interglacial deposit should give the age of the ice sheet advance that emplaced the till. This observation, as well as the fact that the useful age range of the  $^{26}\text{Al}$ - $^{10}\text{Be}$  pair spans the Pleistocene, suggested that  $^{26}\text{Al}$ - $^{10}\text{Be}$  burial dating could significantly improve dating and correlation of Plio-Pleistocene continental glacial sequences. In this paper, we: i) describe the basic principles of cosmogenic-nuclide burial dating; ii) summarize previously published attempts to apply  $^{26}\text{Al}$ - $^{10}\text{Be}$  burial dating to glacial sediment sequences, and explain why they were not always successful; iii) offer an improved method based on the idea of measuring  $^{26}\text{Al}$  and  $^{10}\text{Be}$  concentrations in multiple samples whose exposure histories are linked in some way, and show how this method overcomes previous limitations of burial dating and can be applied in a much wider range of geologic situations; and iv) demonstrate the method by dating the sequence of Plio-Pleistocene tills in an example field area in Missouri.

#### EXAMPLE FIELD AREA: THE MISSOURI TILL-PALEOSOL SEQUENCE

The glacial stratigraphic sequence in central Missouri consists of five distinct and regionally correlated tills separated by paleosols. The till-paleosol sequence is extensively exposed by clay mining operations targeting underlying kaolinite, and the tills and their correlation are described in detail by Rovey and Kean (1996) and Rovey and Tandarich (2006). The lowest till, the Atlanta Formation, overlies deeply weathered preglacial regolith and colluvium, and was emplaced 2.5 Ma (Balco and others, 2005a; this differs from the value of 2.4 Ma stated in that paper because of a recent revision of the  $^{10}\text{Be}$  half-life, as discussed below). The Atlanta till is overlain by, in ascending stratigraphic order, the Moberly, Fulton, Columbia, and Macon tills (fig. 1). The Moberly till is magnetically reversed, indicating deposition prior to 0.78 Ma, and the other three overlying tills have normal polarity. At most sites in Missouri, the till

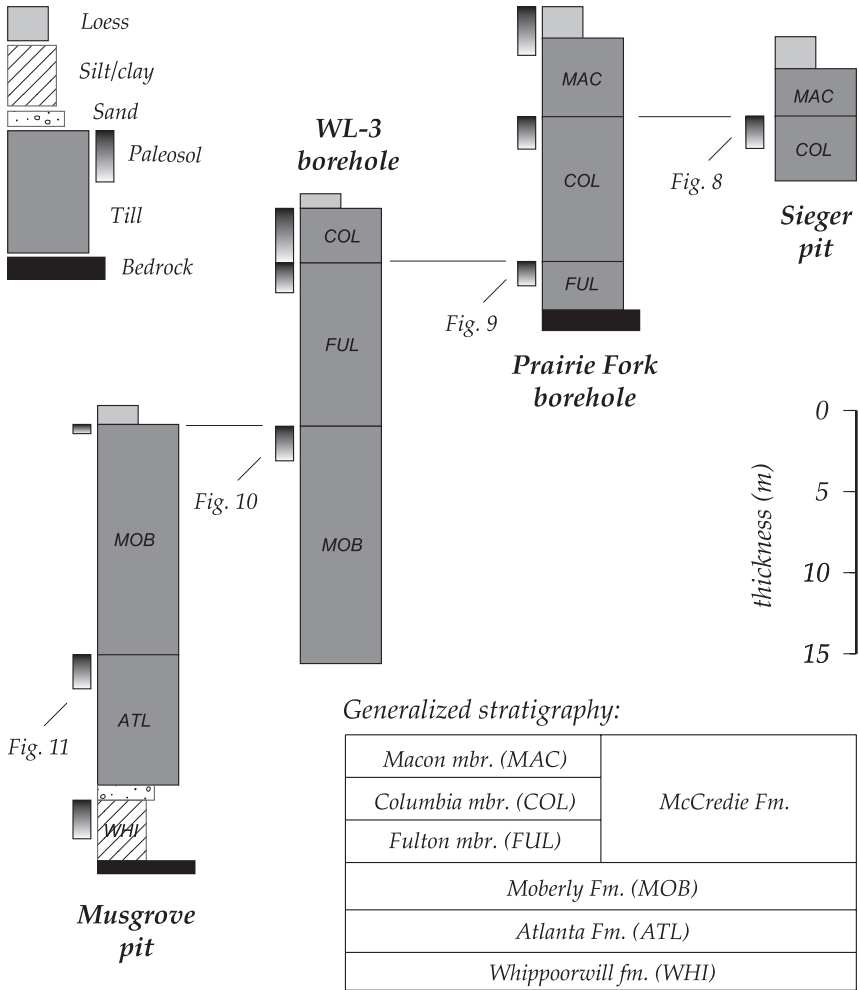


Fig. 1. Generalized stratigraphy of Missouri tills and stratigraphy of the paleosol sites.

sequence is overlain by thin loess. Regional correlations of the loess stratigraphy, as well as observations of weathering profiles developed in the loess and underlying till (Rovey, 1997), indicate that: i) both Wisconsinan (marine oxygen isotope stage 2; ~25 ka) and Illinoian (marine oxygen isotope stage 6; ~150 ka) loesses are present, and ii) a paleosol underlying the Illinoian loess reflects soil formation during the so-called ‘Yarmouth’ interglaciation (marine oxygen isotope stage 7; ~200 ka).

To summarize, existing age control on the Missouri tills indicates only that the Moberly till was deposited between 2.5 Ma and 0.78 Ma, and the Fulton, Columbia, and Macon tills were deposited between 0.78 Ma and ~0.2 Ma. In this paper, we date these four tills directly using <sup>26</sup>Al and <sup>10</sup>Be measurements on quartz grains from the paleosols that underlie them. In the rest of the paper, we will refer to the paleosols by the name of the tills in which they are developed, that is, the Atlanta paleosol is developed on the surface of the Atlanta till and underlies the Moberly till; the Moberly paleosol is developed on the Moberly till and underlies the Fulton till, and so on. To determine the age of the Moberly, Fulton, Columbia, and Macon tills, therefore, we

TABLE 1  
*Site locations*

Site	N Latitude (DD)	W Longitude (DD)	Elevation (m)	Description
Sieger Pit	39.248	91.806	233	Open-pit clay mine
PF2	38.904	91.743	255	Borehole
WL3	38.745	90.990	256	Borehole
Musgrove Pit	38.863	91.437	253	Open-pit clay mine

collected samples from the Atlanta, Moberly, Fulton, and Columbia paleosols, respectively. Table 1 gives the site locations and table 2 summarizes the stratigraphy overlying the paleosol we sampled at each site.

ANALYTICAL METHODS

*<sup>26</sup>Al and <sup>10</sup>Be Measurements*

Paleosol samples consisted of till collected from both boreholes and open-pit clay mines. We extracted medium to coarse sand (0.25–0.85 mm) by disaggregating in water and wet-sieving, then isolated quartz grains by carbonate dissolution in HNO<sub>3</sub> or HCl, repeated etching in dilute HF, and separation of refractory heavy minerals using LST heavy liquid. Al concentrations in the resulting quartz separates were mostly in the range of 40 to 90 ppm. We extracted Al and Be from the quartz separates by standard methods of HF dissolution and column chromatography (see Stone, 2004), determined total Al concentrations by ICP optical emission spectrophotometry on aliquots of the dissolved sample, and measured Al and Be isotope ratios by accelerator mass spectrometry at the Center for Accelerator Mass Spectrometry at Lawrence Livermore

TABLE 2  
*Stratigraphy overlying Missouri paleosols*

Site	Sieger Pit	PF2	WL3	Musgrove Pit
Paleosol	Columbia	Fulton	Moberly	Atlanta
Overlying till	Macon	Columbia	Fulton	Moberly
Loess thickness (m)	0.6	1.9	Absent	3
Macon till				
Thickness (m)	5.3	6.1	Absent	Absent
Dry density (g cm <sup>-3</sup> )	1.86 ± 0.05 (n=2)	1.91 ± 0.05 (n=3)		
Columbia till				
Thickness (m)		5.9	4.6	Absent
Dry density (g cm <sup>-3</sup> )		2.04 ± 0.05 (n=2)	n.m.	
Fulton till				
Thickness (m)			9.6	Absent
Dry density (g cm <sup>-3</sup> )			2.11 ± 0.03 (n = 4)	
Moberly till				
Thickness (m)				11.6
Dry density (g cm <sup>-3</sup> )				1.98 ± 0.07 (n=2)

TABLE 3  
*Analytical*

Sample name	Depth below paleosol surface (cm)		Dry density <sup>1</sup> (g cm <sup>-3</sup> )	Nuclide concentrations in quartz		
	Top	Bottom		[ <sup>10</sup> Be] <sup>2</sup>	[ <sup>10</sup> Be] <sup>3</sup>	[ <sup>26</sup> Al] <sup>4</sup>
				(10 <sup>4</sup> atoms g <sup>-1</sup> )	(10 <sup>4</sup> atoms g <sup>-1</sup> )	(10 <sup>4</sup> atoms g <sup>-1</sup> )
Atlanta paleosol at Musgrove pit						
MO-MP-04-0	0	20	1.81	21.48 ± 0.55	19.43 ± 0.49	68.5 ± 3.2
MO-MP-04-40	40	60	1.95	12.25 ± 0.41	11.08 ± 0.37	37.1 ± 2.5
MO-MP-04-80	80	100	2.15	9.85 ± 0.25	8.90 ± 0.23	29.0 ± 2.6
MO-MP-04-150	150	170	2.12	10.46 ± 0.40	9.46 ± 0.36	30.5 ± 2.0
MO-MP-04-250	250	270	1.94	12.78 ± 0.36	11.55 ± 0.32	31.2 ± 2.2
Moberly paleosol in WL3 borehole						
WL3-45.5-46.5	0	30	1.98	25.25 ± 0.83	22.83 ± 0.75	97.4 ± 4.7
WL3-48-48.75	76	99	1.96	29.23 ± 0.77	26.43 ± 0.70	118.5 ± 5.5
WL3-50-51	137	168	2.06	10.68 ± 0.33	9.66 ± 0.30	40.7 ± 2.3
WL3-52-53	198	229	1.96	8.46 ± 0.21	7.65 ± 0.19	31.6 ± 1.7
WL3-63-64	533	564	2.03	6.86 ± 0.16	6.21 ± 0.15	23.2 ± 1.7
WL3-81-82	1082	1113	2.09	6.18 ± 0.20	5.59 ± 0.18	21.1 ± 1.8
Fulton paleosol in PF2 borehole						
PF2-45.75-48	0 <sup>5</sup>	69 <sup>5</sup>	1.95 <sup>6</sup>	23.8 ± 0.61	21.52 ± 0.55	92.7 ± 4.4
PF2-48.75-52	91 <sup>5</sup>	191 <sup>5</sup>	"	22.67 ± 0.49	20.50 ± 0.45	89.9 ± 4.5
PF2-52-53.5	191	236	"	23.10 ± 0.46	20.89 ± 0.42	92.8 ± 4.7
PF2-53.5-55	236	282	"	17.74 ± 0.43	16.04 ± 0.39	61.9 ± 4.2
Columbia paleosol at Sieger pit						
SP-COL-0	0	15	1.68	17.02 ± 0.33	15.39 ± 0.30	88.4 ± 3.7
SP-COL-1	30	46	1.82	8.82 ± 0.23	7.98 ± 0.21	42.0 ± 2.2
SP-COL-2	61	76	1.88	8.30 ± 0.21	7.51 ± 0.19	39.2 ± 2.0
SP-COL-3	91	107	1.90	8.15 ± 0.21	7.36 ± 0.19	43.1 ± 2.5
SP-COL-5	152	168	1.95	9.63 ± 0.28	8.71 ± 0.25	45.3 ± 2.5

<sup>1</sup> The density measurements have a precision of approximately 0.1 g cm<sup>-3</sup>.

<sup>2</sup> Normalized to the reference standards of Nishiizumi (2002).

<sup>3</sup> Normalized to the reference standards of Nishiizumi (2007).

<sup>4</sup> Normalized to the reference standards of Nishiizumi (2004).

<sup>5</sup> Depth range of cored interval. Sample recovery was incomplete.

<sup>6</sup> Not measured. Average value for the same paleosol at a different site.

National Laboratory. Total carrier and process blanks varied between  $3400 \pm 2300$  and  $10500 \pm 7700$  atoms <sup>10</sup>Be and between  $23000 \pm 23000$  and  $65400 \pm 50000$  atoms <sup>26</sup>Al, and were always less than 1 percent of the total number of atoms measured (these, like all other uncertainties reported in this paper, are 1σ uncertainties). Table 3 and figure 2 show the resulting measured <sup>26</sup>Al and <sup>10</sup>Be concentrations.

#### *Note on <sup>10</sup>Be Measurement Standardization and Decay Constants*

<sup>26</sup>Al and <sup>10</sup>Be measurements in the existing literature have been made against a variety of reference standards that are in some cases inconsistent with each other. Nishiizumi and others (2007) and Nishiizumi (2004) describe this situation in detail. The <sup>10</sup>Be measurements in this paper were originally referenced either to the standards described in Nishiizumi (2002) or those described in Nishiizumi and others

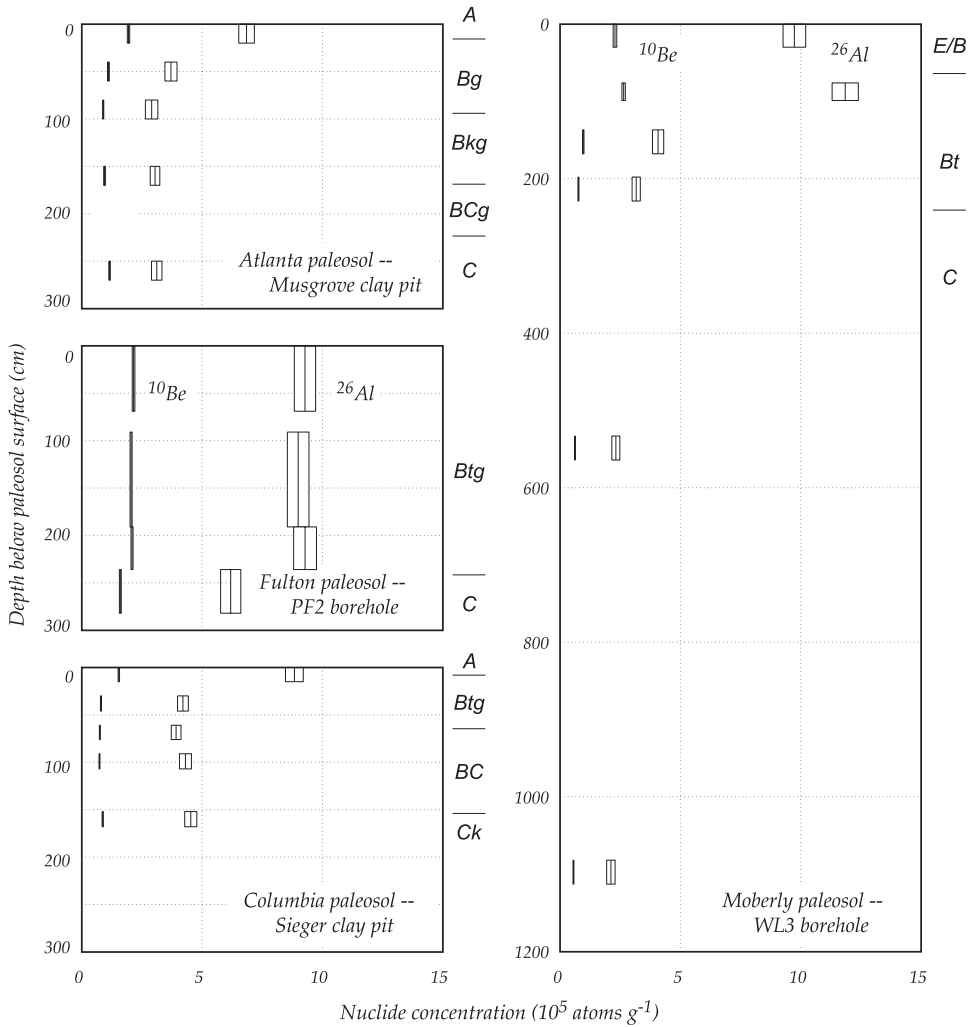


Fig. 2. Soil stratigraphy and  $^{26}Al$  and  $^{10}Be$  concentrations in Missouri paleosols. The height of the boxes shows the depth range over which each sample was collected; the width of the boxes is the  $1\sigma$  uncertainty of the  $^{26}Al$  and  $^{10}Be$  measurements. Soil horizons are indicated at the right of each panel.

(2007); here, we have renormalized all the  $^{10}Be$  measurements to the Nishiizumi and others (2007) standards ( $^{10}Be$  concentrations referenced to both standards are shown in table 3).  $^{26}Al$  measurements are referenced to the standards described in Nishiizumi (2004). Each set of reference standards implies a particular value for the corresponding decay constant; thus, in this paper we use the  $^{10}Be$  decay constant of  $5.10 \pm 0.26 \times 10^{-7} \text{ yr}^{-1}$  from Nishiizumi and others (2007), and the  $^{26}Al$  decay constant of  $9.83 \pm 0.25 \times 10^{-7} \text{ yr}^{-1}$  from Nishiizumi (2004). This means that burial ages given in this paper are inconsistent with those given in publications that adopted the  $^{10}Be$  decay constant of Nishiizumi (2002), specifically, all of our previous work (Balco and others, 2005a, 2005b, 2005c). In general, given the same set of measurements, a burial age calculated using the  $^{10}Be$  standardization and decay constant of Nishiizumi and others (2007) will be approximately 10 percent older than one calculated using the  $^{10}Be$

standardization and decay constant of Nishiizumi (2002). We call further attention to this issue when referring to previous work throughout this paper.

#### DATA-REDUCTION METHODS I: REVIEW OF PREVIOUS APPLICATIONS OF BURIAL DATING

Although burial dating is in principle possible with any pair of cosmogenic radionuclides that are produced at a fixed ratio in a particular mineral but have different half-lives, nearly all terrestrial applications of burial dating have used the  $^{26}\text{Al}$ - $^{10}\text{Be}$  pair.  $^{26}\text{Al}$  and  $^{10}\text{Be}$  are produced in quartz at a ratio of 6.75:1 [Note that this value is commonly stated as 6.1:1 (Nishiizumi and others, 1989). It depends on the reference standards used for  $^{26}\text{Al}$  and  $^{10}\text{Be}$  measurements, as discussed above].  $^{10}\text{Be}$  has a half-life of 1.36 Myr and  $^{26}\text{Al}$  has a half-life of 0.705 Myr, giving a useful time range for  $^{26}\text{Al}$ - $^{10}\text{Be}$  burial dating of approximately 0.2 to 4 Ma. Burial dating by  $^{26}\text{Al}$  and  $^{10}\text{Be}$  is straightforward when the sample in question has experienced a two-stage exposure history only: that is, it originated from steady erosion of a surface that was exposed for a long enough time that surface nuclide concentrations came to equilibrium with the long-term erosion rate, it was buried at a sufficient depth to largely stop the cosmic-ray flux, and it remained buried at that depth until the present time. In this situation, the  $^{26}\text{Al}$  and  $^{10}\text{Be}$  concentrations measured in the sample at the present time are:

$$N_{10,m} = \frac{P_{10}(0)}{\varepsilon} e^{-\lambda_{10}t_b} + \frac{P_{10}(z_b)}{\lambda_{10}} [1 - e^{-\lambda_{10}t_b}] \quad (1)$$

$$\lambda_{10} + \frac{\Lambda}{\varepsilon}$$

$$N_{26,m} = \frac{P_{26}(0)}{\varepsilon} e^{-\lambda_{26}t_b} + \frac{P_{26}(z_b)}{\lambda_{26}} [1 - e^{-\lambda_{26}t_b}] \quad (2)$$

$$\lambda_{26} + \frac{\Lambda}{\varepsilon}$$

where  $N_{i,m}$  is the measured concentration of nuclide  $i$  at the present time (atoms  $\text{g}^{-1}$ ),  $P_i(0)$  is the surface production rate of nuclide  $i$  (atoms  $\text{g}^{-1} \text{yr}^{-1}$ ),  $\lambda_i$  is the decay constant for nuclide  $i$ ,  $z_b$  is the burial depth of the sample ( $\text{g cm}^{-2}$ ),  $P_i(z_b)$  is the production rate (atoms  $\text{g}^{-1} \text{yr}^{-1}$ ) at the burial depth of the sample,  $\varepsilon$  is the surface erosion rate prior to burial ( $\text{g cm}^{-2} \text{yr}^{-1}$ ),  $t_b$  is the duration of burial (yr), and  $\Lambda$  is the effective attenuation length for spallogenic production (here taken to be  $160 \text{ g cm}^{-2}$ ). Throughout this paper we use ‘mass depth,’ the product of linear depth (cm) and density ( $\text{g cm}^{-3}$ ), to describe depth below the surface. This reflects the importance of mass, rather than distance, in attenuating the cosmic-ray flux, and simplifies the mathematical expressions. The first term on the right-hand side of these equations is the formula for the nuclide concentration in a steadily eroding surface (Lal, 1991), with a radioactive decay factor applied to correct it to the present time; the second term is the post-burial nuclide inventory, that is, the amount of  $^{26}\text{Al}$  or  $^{10}\text{Be}$  produced in the sample between the time of burial and the present. If the sample is deeply buried (so that the post-burial nuclide production is small) and the burial time is not significantly longer than the  $^{26}\text{Al}$  and  $^{10}\text{Be}$  half-lives (so that the nuclide concentration in the sample at the time of burial has not decayed away completely), then the second term is significantly smaller than the first term. Given the sample depth, the measured  $^{26}\text{Al}$  and  $^{10}\text{Be}$  concentrations, a knowledge of the nuclide production-depth function  $P(z)$ , and the decay constants, this pair of equations can be solved to yield the surface erosion rate  $\varepsilon$  and the burial age  $t_b$ . The additional assumptions that i) the post-burial production is infinitesimally small, and ii) the erosion rate is fast enough that radioactive decay during the period of erosion can be neglected, yield an approximate



solution that shows the basic relationship between the burial age  $t_b$  and  $R_m$ , the  $^{26}\text{Al}/^{10}\text{Be}$  ratio measured at the present time:

$$R_m = \frac{N_{26,m}}{N_{10,m}} = \frac{P_{26}(0)}{P_{10}(0)} e^{-t_b(\lambda_{26} - \lambda_{10})} \quad (3)$$

At the time of burial ( $t_b = 0$ ), the  $^{26}\text{Al}/^{10}\text{Be}$  ratio in the sample is equal to the production ratio; once buried, it decreases exponentially at a rate controlled by the  $^{26}\text{Al}$  and  $^{10}\text{Be}$  decay constants. To summarize, the simplest application of two-nuclide burial dating involves a single sample whose geological context shows that it has experienced a single period of steady erosion and a single period of burial, so equations (1) and (2) apply. Henceforth we will refer to an  $^{26}\text{Al}$ - $^{10}\text{Be}$  burial age calculated using equations (1) and (2) as a 'simple burial age.'

Equations (1) and (2) apply in the primary existing application of burial dating, that is, to cave sediments which were derived from steady surface erosion, deposited in the cave, and therefore shielded from further cosmogenic-nuclide production. Here the geologic history of the samples is clearly consistent with the assumptions needed to apply equations (1) and (2), and the simple burial age of these samples accurately reflects their depositional age. In previous work (Balco and others, 2005a), we were also able to use the simple burial dating approach to date the stratigraphically lowest till in Missouri, the Atlanta Formation, where this till overlies quartz-bearing colluvium derived from slow erosion of the local landscape prior to glaciation. In this situation, the colluvium was buried in place by till deposition, rather than being carried into a cave, but the basic sequence of events is the same. Thus, equations (1) and (2) apply, and the burial age of the colluvium dates the emplacement of the till.

The major disadvantage of the simple burial dating approach is that it cannot accommodate the geologically common circumstance where the sample has experienced a complex exposure history prior to burial. For example, in a glacial sequence where a paleosol developed in one till is buried by a second till, the quartz in the lower till that forms the paleosol parent material did not necessarily experience only a single period of steady erosion prior to burial. It could have arrived at the site with inherited  $^{26}\text{Al}$  and  $^{10}\text{Be}$  concentrations reflecting an unknown, and potentially complicated, history of surface exposure, burial, and mixing of older sediment from different sources. Thus, the  $^{26}\text{Al}/^{10}\text{Be}$  ratio in paleosol quartz at the time the paleosol was buried by the upper till would reflect not only the  $^{26}\text{Al}/^{10}\text{Be}$  ratio of 'new'  $^{26}\text{Al}$  and  $^{10}\text{Be}$  produced during soil formation (which would conform to the production ratio), but also the ratio of the inherited  $^{26}\text{Al}$  and  $^{10}\text{Be}$  inventories (which might not conform to the production ratio). As we do not know the exposure history of the quartz incorporated in the till, we do not know its inherited  $^{26}\text{Al}/^{10}\text{Be}$  ratio. This in turn means that we have no constraint on the  $^{26}\text{Al}/^{10}\text{Be}$  ratio at the time of burial, which invalidates the assumptions involved in calculating a simple burial age. In other words, this adds two additional unknowns (the inherited  $^{26}\text{Al}$  and  $^{10}\text{Be}$  concentrations) to equations (1) and (2), precluding a unique solution. In another previous paper (Balco and others, 2005b), we showed that glacial and interglacial sediments in the north-central US are in fact derived from the erosion, transport, and redeposition of older glacial deposits that themselves had a long history of repeated exposure, burial, and recycling. They contain large and highly variable amounts of inherited  $^{26}\text{Al}$  and  $^{10}\text{Be}$ , always with an  $^{26}\text{Al}/^{10}\text{Be}$  ratio well below the production ratio. Staiger and others (2006) also noted this. These observations show that the simple burial age of a paleosol developed in one till and overlain by another till will, in general, seriously overestimate the depositional age of the upper till.

In a third previous paper (Balco and others, 2005c), we exploited two observations to develop a method of separating inherited  $^{26}\text{Al}$  and  $^{10}\text{Be}$  from  $^{26}\text{Al}$  and  $^{10}\text{Be}$



produced during soil formation. First, till is commonly massive and lithologically homogeneous at spatial scales from meters to kilometers, indicating that it is well mixed by subglacial deformation. If the paleosol parent material is massive till, we may not know what the inherited  $^{26}\text{Al}$  and  $^{10}\text{Be}$  concentrations are, but we know that they are the same at all depths in the soil. Second, the depth-concentration relationship of  $^{26}\text{Al}$  and  $^{10}\text{Be}$  produced during soil formation can be predicted from the surface concentration and the known depth dependence of the production rate. These observations imply that the depth-nuclide concentration relationship in the paleosol at the time of burial is a function of two parameters: the inherited nuclide concentration in the soil parent material and the surface concentration attributable to exposure during soil formation. By analyzing samples at multiple depths to determine the depth-concentration profile, one can solve for these two parameters uniquely. Anderson and others (1996) introduced this idea in a method for dating river terraces using both the  $^{10}\text{Be}$  concentration of surface gravel and the  $^{10}\text{Be}$  concentration of subsurface gravel collected in a soil pit. In Balco and others (2005c), we applied it in the context of burial dating by using depth profiles of  $^{10}\text{Be}$  and  $^{26}\text{Al}$  in a paleosol to determine the inherited  $^{26}\text{Al}$  and  $^{10}\text{Be}$  concentrations in the paleosol parent material. We could then disregard these inherited nuclide concentrations in calculating the burial age, thus satisfying the assumptions of simple burial dating. In order to account for additional complicating factors such as changes in the burial depth with time, we applied this idea using a forward modeling approach that predicts the expected depth-nuclide concentration relationships for  $^{26}\text{Al}$  and  $^{10}\text{Be}$  in a paleosol that was developed on a parent material with some inherited nuclide concentration, was exposed for a time without surface erosion, and then was buried until the present time. The model has four parameters: the inherited  $^{26}\text{Al}$  and  $^{10}\text{Be}$  concentrations, the exposure time, and the burial time. In Balco and others (2005c), we measured  $^{26}\text{Al}$  and  $^{10}\text{Be}$  concentrations at multiple depths in a paleosol overlain by loess in a borehole in eastern Nebraska, and computed best-fitting values for these parameters using a numerical optimization method. Figure 3 reproduces the  $^{26}\text{Al}$  and  $^{10}\text{Be}$  measurements in this paper and shows the results of fitting model depth-concentration profiles to the data. It is clear that the model profiles are a good fit to the measurements at this site, and the fitting exercise yielded a well-constrained burial age.

Encouraged by this success, we sought to apply this method to additional till-paleosol sequences in Missouri. We were not successful, because of a significant weakness in the forward model approach. Fitting measured nuclide concentrations at certain depths with a forward model assumes that: a) we know the precise depths relative to the soil surface at which the quartz grains in our samples resided during soil formation and nuclide production, and b) these depths did not change during soil formation or burial. Unfortunately, common geologic processes invalidate these assumptions. Nearly all soils undergo processes such as vertical mixing by bioturbation or pedoturbation, inflation by windblown sediment, and deflation due to dissolution of easily weatherable minerals. All of these processes would act to move quartz grains up and down in the soil, resulting in a nuclide concentration-depth relationship that would not resemble the production rate-depth relationship. We were lucky in the Nebraska example in Balco and others (2005c) and figure 3 to have found a paleosol where these mixing processes were apparently confined to a zone near the surface that was thinner than our uppermost sample, did not disturb the smooth exponential profile predicted by the forward model, and thus could be safely disregarded. This conclusion, that this soil experienced little vertical mixing during soil formation, is a surprising result of the good agreement between the measurements and the model prediction. Figure 2 shows that it does not apply to other soils. None of the depth-nuclide concentration profiles in the Missouri paleosols described in this paper

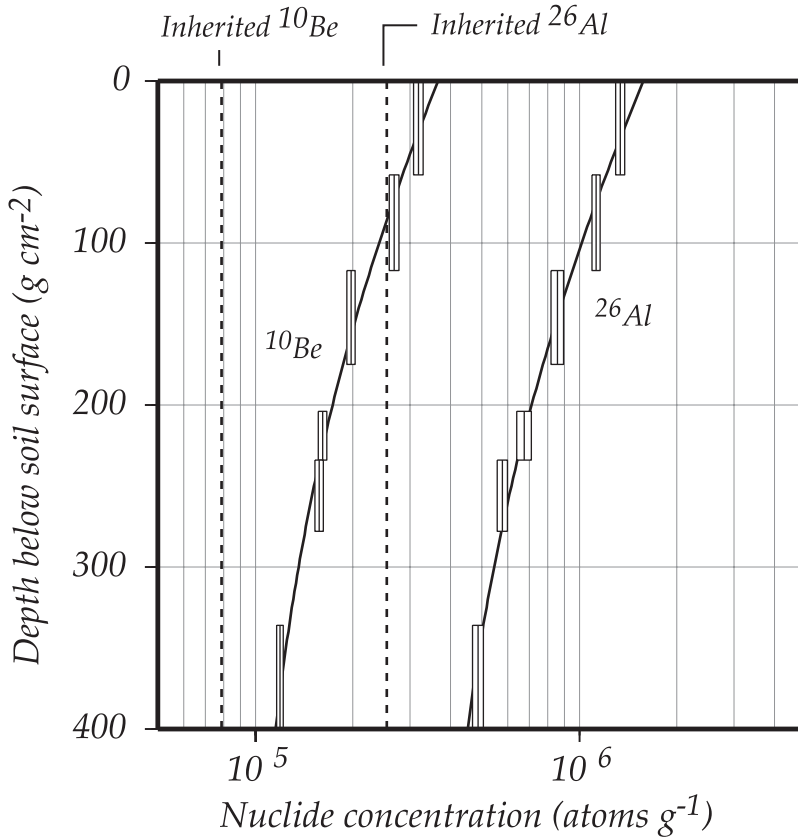


Fig. 3.  $^{26}\text{Al}$  and  $^{10}\text{Be}$  concentrations in a paleosol in the 3-B-99 borehole in eastern Nebraska described in Balco and others (2005c). The height of the boxes shows the depth range over which each sample was collected; the width of the boxes is the  $1\sigma$  uncertainty of the  $^{26}\text{Al}$  and  $^{10}\text{Be}$  measurements. The dark lines show the results of fitting the forward model described in Balco and others (2005c) to the data. In this case, the model fits the data very well. Comparison with the concentration-depth profiles measured in the Missouri paleosols (fig. 2) shows that a model of this form would not accurately fit those data.

resemble the smooth exponential profiles predicted by the forward model of Balco and others (2005c). All the soil-forming processes noted above that could cause divergence of the actual nuclide concentration-depth profile from the production rate-depth profile are probably represented in this data set. In principle, we could include some of these processes in the forward model and continue trying to determine the burial age by fitting the measured depth profiles, but in practice this would result in a proliferation of unknown parameters that describe poorly quantified processes, effectively eliminating the possibility of solving for a unique burial age. Furthermore, many of the paleosols that we sampled in this study—again unlike the Nebraska example—have been affected by subglacial deformation during emplacement of the tills that bury them. In these cases, we do not even have any way to know what depth the samples resided at before they were buried. Finally, in the case of samples collected from drillcore, core compaction or incomplete recovery can further confuse the vertical relationship of the samples.

To summarize, the observations that i) nearly all paleosols buried by tills appear to have experienced vertical mixing due to soil-forming processes, subglacial deforma-

tion, or both, and ii) it is not always possible to collect undisturbed drill core through these paleosols, are fatal to any method that relies on forward modeling of the nuclide concentration at specific depths in the paleosol. The forward modeling method can deal with the problem of unknown inherited nuclide concentrations in the soil parent material in the special case where vertical mixing of the soil can be disregarded, but fails in the general case where it cannot be disregarded. Thus, to date till-paleosol sequences in general, we need a method where the burial age can be determined without knowing either the inherited nuclide concentrations in the soil parent material or the precise time-depth history of each sample. In the rest of this paper, we: i) describe a method for dating till-paleosol sequences that meets these criteria, ii) discuss how the method can be adapted to work in other stratigraphic situations as well, and iii) use the method to date the Missouri till-paleosol sequence.

#### DATA-REDUCTION METHODS II: AN ISOCHRON METHOD FOR BURIAL DATING OF PALEOSOLS

In this section, we describe a method for dating till-paleosol sequences that allows us to determine the burial age of paleosols from the  $^{26}\text{Al}$  and  $^{10}\text{Be}$  concentrations in quartz at different depths in the paleosol, without knowing either the inherited  $^{26}\text{Al}$  and  $^{10}\text{Be}$  concentrations in the paleosol parent material or the time-depth history of the samples. In the next section, we describe how a similar method can be used in other stratigraphic situations where the geologic context leads to a different set of assumptions. Here we will: i) start with a set of assumptions derived from geological evidence, ii) use these assumptions to construct a relationship between the burial age of the paleosol and the  $^{26}\text{Al}$  and  $^{10}\text{Be}$  concentrations in the paleosol, iii) use this relationship to develop a sampling strategy that will allow us to uniquely determine the burial age from the measurements, and iv) describe the mathematical implementation of the method in detail.

#### *The Basic Idea*

For clarity in the mathematical description, we will start with a simplified description of the exposure history of quartz in a paleosol developed on one till and buried by a second till. The lower till is well-mixed, so quartz in this till contains unknown but spatially uniform concentrations of  $^{10}\text{Be}$  and  $^{26}\text{Al}$  inherited from prior exposure of the till source material. The presence of a paleosol shows that the lower till was exposed at the surface for a time; the duration of the exposure period is  $t_e$  (yr). The period of surface exposure is followed by burial of the paleosol under a second till; the duration of burial is  $t_b$  (yr). We simplify the situation by assuming that there is no surface erosion, that the exposure time is short enough that we can disregard radioactive decay during the period of exposure, that nuclide production by muons is negligible, and that the overlying till is thick enough that post-burial nuclide production is negligible. With these assumptions, the measured  $^{26}\text{Al}$  and  $^{10}\text{Be}$  concentrations in the soil that we would measure at the present time are:

$$N_{10,m} = [N_{10,inh} + P_{10}(0)t_e e^{-Z/\Lambda}]e^{-t_b\lambda_{10}} \quad (4)$$

$$N_{26,m} = [N_{26,inh} + P_{26}(0)t_e e^{-Z/\Lambda}]e^{-t_b\lambda_{26}} \quad (5)$$

where  $N_{10,inh}$  and  $N_{26,inh}$  are the inherited  $^{10}\text{Be}$  and  $^{26}\text{Al}$  concentrations (atoms  $\text{g}^{-1}$ ) present in the lower till at the time it was emplaced, that is, at the beginning of soil formation.  $Z$  ( $\text{g cm}^{-2}$ ) is depth below the paleosol surface. The other symbols are as described above.

These equations describe  $^{26}\text{Al}$  and  $^{10}\text{Be}$  concentrations in the paleosol as a function of depth below the paleosol surface. However, we want a formula for the burial age of the soil that does not depend on the sample depth. Thus, we eliminate the

depth term  $e^{-z/\Lambda}$  to give a relation between the  $^{26}\text{Al}$  and  $^{10}\text{Be}$  concentrations in a sample that is true at all depths. Equation (4) yields:

$$e^{-z/\Lambda} = \frac{e^{t_b\lambda_{10}}N_{10,m} - N_{10,inh}}{P_{10}(0)t_e} \quad (6)$$

Substituting equation (6) into equation (5),

$$N_{26,m} = e^{-t_b\lambda_{26}}N_{26,inh} + R_{init}e^{-t_b\lambda_{26}}(e^{t_b\lambda_{10}}N_{10,m} - N_{10,inh}) \quad (7)$$

$$N_{26,m} = R_{init}e^{-t_b(\lambda_{26}-\lambda_{10})}N_{10,m} + [e^{-t_b\lambda_{26}}N_{26,inh} - R_{init}e^{-t_b\lambda_{26}}N_{10,inh}] \quad (8)$$

$R_{init}$  is the  $^{26}\text{Al}/^{10}\text{Be}$  ratio at the time the paleosol is buried. With the simplifying assumptions noted above,  $R_{init}$  is equal to  $P_{26}(0)/P_{10}(0)$ , the spallogenic  $^{26}\text{Al}/^{10}\text{Be}$  production ratio. Equation (8) is a linear relation between  $^{10}\text{Be}$  and  $^{26}\text{Al}$  concentrations that is true at all depths. If we were to analyze a set of samples from arbitrary, but different, depths, their  $^{10}\text{Be}$  and  $^{26}\text{Al}$  concentrations would lie on this line. It passes through the point  $(N_{10,inh}e^{-t_b\lambda_{10}}, N_{26,inh}e^{-t_b\lambda_{26}})$  and has slope  $R_{init}e^{-t_b(\lambda_{26}-\lambda_{10})}$ .

The important thing about this relation is that we know the production ratio and the decay constants, so the slope of the line depends only on the burial age  $t_b$ . Thus, we do not need any information about the sample depths, the exposure time, or the inherited nuclide concentrations to determine the burial age of the soil. We need only analyze samples from a range of depths in the paleosol, plot the measured  $^{26}\text{Al}$  and  $^{10}\text{Be}$  concentrations in  $^{10}\text{Be}$ - $^{26}\text{Al}$  space, and determine the slope of the line passing through them. Figure 4 shows this graphically. If this measured slope is  $R_M$ , the burial age of the soil is:

$$t_b = \frac{-\ln(R_M/R_{init})}{(\lambda_{26} - \lambda_{10})} \quad (9)$$

Note that this equation is equivalent to equation (3), which gives the simple burial age of a single sample under the same assumptions of brief exposure, zero erosion, and negligible post-burial production. The simple burial age approach assumes that nuclide inheritance is zero, so the isochron would pass through the origin,  $R_M$  would simply be the measured  $^{26}\text{Al}/^{10}\text{Be}$  ratio in the sample, and it would not be necessary to measure samples at multiple depths to determine the burial age (fig. 4). In the general case where the samples inherit an unknown amount of  $^{10}\text{Be}$  and  $^{26}\text{Al}$ , the isochron does not necessarily pass through the origin, so  $R_M$  is not necessarily equal to the measured  $^{26}\text{Al}/^{10}\text{Be}$  ratio in any of the samples, and several samples collected at different depths are needed to determine it.

One interesting aspect of this approach is that the  $[^{10}\text{Be}] - [^{26}\text{Al}]/[^{10}\text{Be}]$  diagram with logarithmic or semi-logarithmic axes, commonly used in nearly all other papers describing burial dating (see Granger, 2006, for details), hides the fact that, no matter what the inherited nuclide concentrations, burial isochrons are straight lines. In that diagram, the apparent curvature of the isochrons varies within the diagram depending on the inherited nuclide concentrations, the burial age, and the normalization used to draw the diagram. We avoid that diagram in the present paper and simply plot  $^{26}\text{Al}$  against  $^{10}\text{Be}$  concentrations on linear axes.

#### *Complications Due to Post-Burial Nuclide Production*

In the previous section we assumed that post-burial nuclide production was negligible. In reality, a paleosol that is buried under several meters of till will still be subject to a low level of  $^{26}\text{Al}$  and  $^{10}\text{Be}$  production by muon interactions. For a deeply buried sample, the production rate at the burial depth may be orders of magnitude

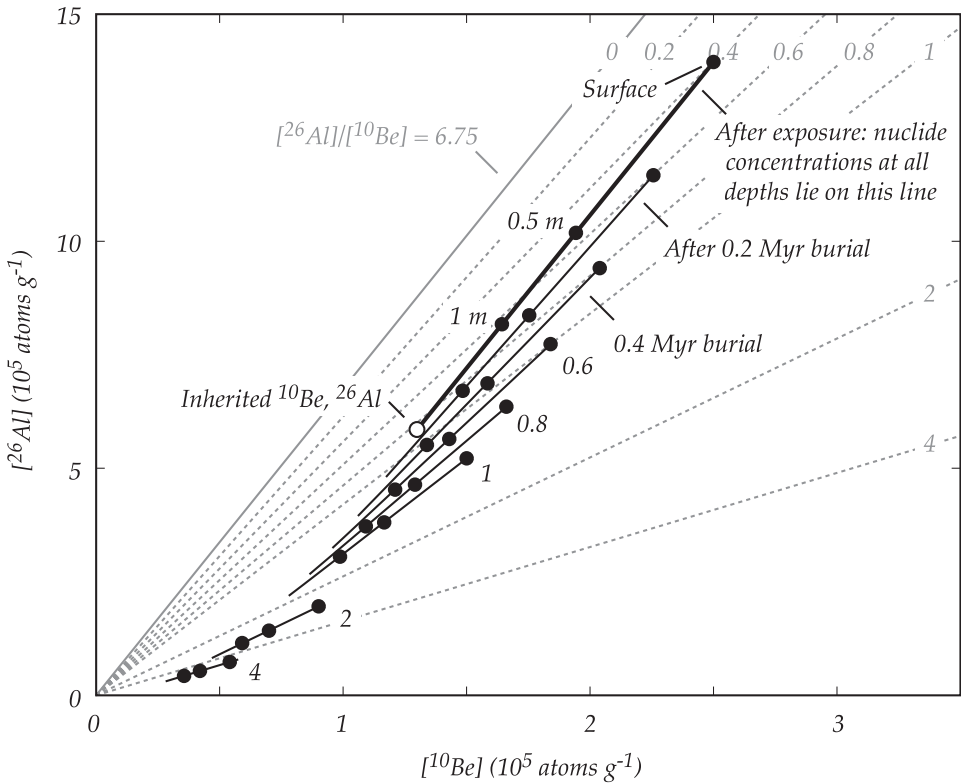


Fig. 4. The idea of a  $^{26}\text{Al}$ - $^{10}\text{Be}$  burial isochron. Quartz in a soil starts out with some arbitrary concentrations of inherited  $^{26}\text{Al}$  and  $^{10}\text{Be}$  (open circle). Nuclide concentrations increase during exposure and soil formation, to a greater extent at shallower depths. After a time, the nuclide concentrations in quartz at different depths will lie along a line whose slope is given by the production ratio (the uppermost dark line). During subsequent burial (at infinite depth in this example), all nuclide concentrations decrease, and the slope of the line connecting nuclide concentrations at different depths in the soil decreases (thinner dark lines). The slope of the line does not depend on the inherited nuclide concentrations, only on the duration of burial. The light lines in the background are contours of the simple burial age—that assumes zero inheritance—inferred from a single sample. Comparing these with the burial isochrons highlights the fact that, when inherited  $^{26}\text{Al}$  and  $^{10}\text{Be}$  have a low  $^{26}\text{Al}/^{10}\text{Be}$  ratio, the simple burial age always overestimates the actual burial age.

lower than the surface production rate. However, the burial age of a paleosol may similarly be orders of magnitude greater than its exposure time, so a substantial fraction of the measured nuclide concentration may be due to production after burial. The importance of this depends on the depth range spanned by the samples, and on how deeply they are buried. The slope of the production rate-depth relationship decreases as the depth increases, so if the samples span a depth range that is small relative to their overall burial depth, then post-burial production is similar for all samples and therefore has a negligible effect on the slope of the isochron. In this case, post-burial production could be disregarded. In our application to till-paleosol sequences, however, this is not the case: we collected samples over a  $\sim 2$  m range in paleosols that are buried by 5 to 20 m of till. Here post-burial production varies significantly between samples, it has a systematic effect on the slope of the isochron, and if we did not account for it, we would obtain an incorrect burial age. The production rate-depth relationship is known to sufficient accuracy that post-burial production can be accounted for by an iterative solution method: First, calculate the

slope of the isochron and thence the burial age assuming burial at infinite depth, that is, no post-burial production. Then, calculate the nuclide concentrations attributable to post-burial production at the actual sample depth during that length of time. Subtract these from the measured nuclide concentrations and recalculate the isochron slope and burial age using the corrected data. Iterate until the result converges on a solution.

In the examples we discuss later, the paleosols we are trying to date are buried by multiple overlying tills. We are treating only the emplacement age of the till immediately overlying the paleosol as an unknown, so we need information about the ages of the tills higher in the section, as well as their surface erosion rates during intervals between ice sheet advances, to properly calculate the post-burial nuclide concentrations. We follow Balco and others (2005a) in accounting for this and use a ‘sawtooth’ age-depth model to calculate nuclide production after burial, in which the burial depth increases instantaneously with deposition of a particular overburden unit, then decreases steadily due to surface erosion until the emplacement of the next overburden unit. In this study, we date all the tills in the section, so if we begin by dating the uppermost till, we can use that information to constrain the latter parts of the age-depth history for paleosols underlying tills lower in the section. We also need an estimate of the surface erosion rate between the emplacement of one till and the next. As discussed below, an estimate of the erosion rate sustained by the paleosol being dated is a byproduct of the age calculation. Erosion rate estimates derived from our measurements in this study were  $\sim 10$  to  $30$  m Myr $^{-1}$ , and the better constrained estimates were  $\sim 10$  to  $20$  m Myr $^{-1}$  (fig. 5). These are larger than early and middle Pleistocene surface erosion rates inferred from burial dates on cave sediments in the central U.S., which are  $1$  to  $10$  m Myr $^{-1}$  (Granger, 2006). Taking all this into account, we used a surface erosion rate between emplacement of overburden units of  $10 \pm 5$  m Myr $^{-1}$  in calculating nuclide production after burial. These erosion rate estimates are not very accurate, but as long as the tills immediately overlying the sampled paleosols are relatively thick, the value assumed for the surface erosion rate between overburden emplacement events has a negligible effect on the burial ages. This is an important point: despite the complexity of this procedure for accounting for post-burial production, and its dependence on a variety of poorly constrained parameters, if the till immediately overlying the paleosol is relatively thick, the variation in post-burial  $^{26}\text{Al}$  and  $^{10}\text{Be}$  production among samples is always much less than the variation in their total nuclide concentrations. Thus, even a large correction for post-burial production results in only a small change to the isochron slope. Large uncertainties in estimating the post-burial production, because either the geologic history or production rates due to muons are not precisely known, result only in small uncertainties in the overall burial age. We discuss this in more detail later in the section on error propagation.

#### *Complications Due to Long Exposure and Erosion Before Burial*

We also assumed above that the paleosol did not erode during its exposure, and that the exposure time was short enough that radioactive decay could be disregarded. This implied that  $R_{init}$ , the slope of the isochron at the time of burial, was simply  $P_{26}(0)/P_{10}(0)$ , the spallogenic production ratio. In the general case,  $R_{init}$  depends on the exposure time and erosion rate during the period of soil formation. For exposure time  $t_e$  and steady erosion rate  $\epsilon$ :

$$R_{init} = \frac{P_{26}(0)(\lambda_{10} + \epsilon/\Lambda)[1 - \exp(-[\lambda_{26} + \epsilon/\Lambda]t_e)]}{P_{10}(0)(\lambda_{26} + \epsilon/\Lambda)[1 - \exp(-[\lambda_{10} + \epsilon/\Lambda]t_e)]} \quad (10)$$

$(t_e, \epsilon)$  pairs that satisfy this equation define the ‘steady state erosion island’ of Lal (1991). Figure 5 shows the variation in  $R_{init}$  with  $t_e$  and  $\epsilon$ . Long exposure times, and



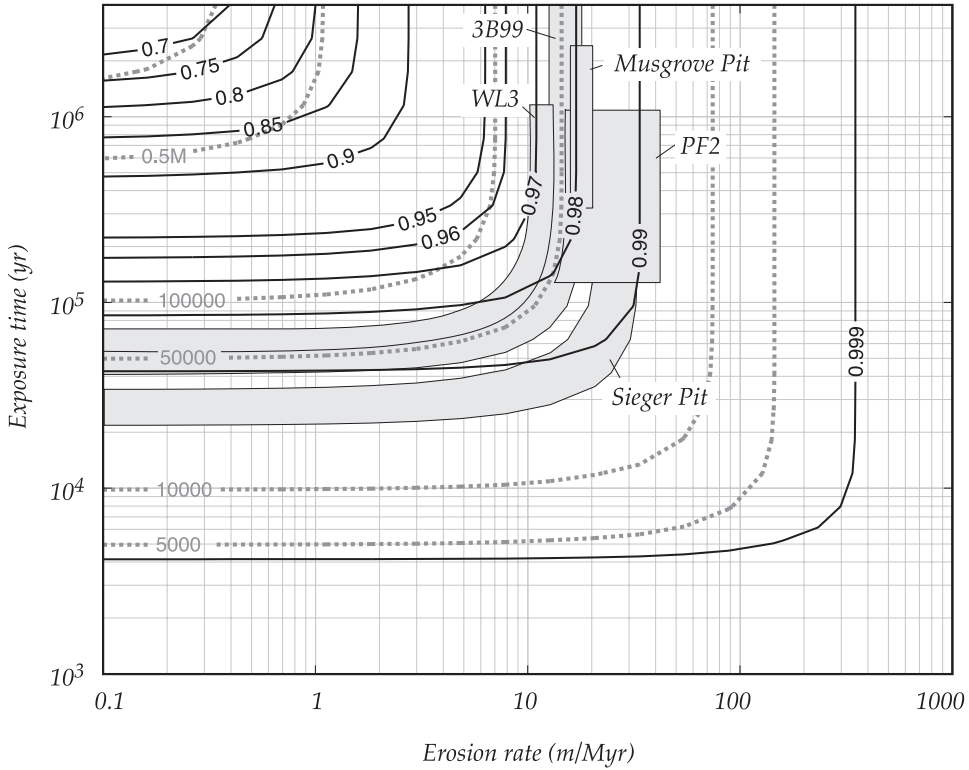


Fig. 5. Effects of extended exposure and surface erosion on the parameter  $R_{init}$ , according to equation (10). The dark lines are contours of the ratio of  $R_{init}$  to the  $^{26}\text{Al}/^{10}\text{Be}$  production ratio  $P_{26}(0)/P_{10}(0)$  as a function of surface erosion rate and exposure time.  $R_{init}$  is close to the production ratio when exposure times are short and/or erosion is rapid, and diverges at long exposure times and low erosion rates as radioactive decay becomes more important. The dotted gray contours show  $^{10}\text{Be}$  concentrations developed during exposure, normalized to the surface production rate (this quantity has units of years, but is more sensibly thought of as the  $^{10}\text{Be}$  concentration in atoms  $\text{g}^{-1}$  given a surface  $^{10}\text{Be}$  production rate of 1 atom  $\text{g}^{-1} \text{yr}^{-1}$ ). Production due to muon interactions is not included in this plot, so it is simply a remapping of the simple exposure island of Lal (1991). The gray regions show the range of exposure ages and erosion rates permitted for the paleosols in this study, inferred from correcting the measured nuclide concentrations back to the time of burial as described in the text. The boundaries of these regions reflect i) the allowable range for the surface  $^{10}\text{Be}$  concentration attributable to surface exposure, and ii) 95% confidence limits on the exposure time of the paleosols obtained from differencing the ages of the overlying till and the till in which the paleosol is developed (for the Missouri tills—there is no constraint on the age of the till in the 3B99 borehole). The important point is that even though our method provides only very weak bounds on the erosion rates and exposure times of the paleosols prior to burial, they are all in a range where the variation in  $R_{init}$  is small, so a large uncertainty in estimating surface production rates, exposure times, and erosion rates translates into only a small uncertainty in estimating  $R_{init}$  and determining the burial age of the paleosol.

likewise slow erosion rates which allow a sample to reside near the surface for the full duration of exposure and accumulate a large nuclide inventory, result in  $R_{init}$  significantly below the production ratio. The value of  $R_{init}$  used in determining the burial age in equation (9) has to be adjusted to account for this effect. Note that we have not considered soil mixing processes that increase the residence time of some quartz grains in the soil more than expected from steady erosion alone, and further decrease  $R_{init}$ . This is a secondary issue for the present purposes; for a mathematical treatment see Lal and Chen (2005).

We account for the dependence of  $R_{init}$  on paleosol exposure time and erosion rate by another iteration scheme, as follows. First, once we have determined both an



initial burial age for the soil and the nuclide concentration attributable to post-burial production, we use these to correct the measured  $^{10}\text{Be}$  concentrations back to their values at the time of burial. Second, we use these corrected  $^{10}\text{Be}$  concentrations to estimate the inherited  $^{10}\text{Be}$  concentration at the time of burial ( $N_{10,inh}e^{-\lambda_{10}t_c}$ ) in the paleosol. We cannot do this explicitly, of course, because the whole point of the isochron method is that we do not know the age-depth history of the samples well enough to determine the inherited nuclide concentrations by fitting a depth-concentration profile to the measurements. However, we can limit the inherited  $^{10}\text{Be}$  concentration by observing that it must be less than the lowest of the corrected  $^{10}\text{Be}$  concentrations in our samples and greater than the x-intercept of a line drawn through the corrected  $^{10}\text{Be}$  and  $^{26}\text{Al}$  measurements. Here it is useful to have analyzed a sample well below the paleosol surface so as to limit the inheritance more closely. Third, subtracting these limiting values of ( $N_{10,inh}e^{-\lambda_{10}t_c}$ ) from the corrected  $^{10}\text{Be}$  concentration in the uppermost sample yields limits on  $N_{10,exp}$ , the surface nuclide concentration attributable to surface exposure during soil formation, at the time of burial. Fourth, each limiting value of  $N_{10,exp}$  can be used to calculate either the apparent exposure age of the soil at burial given zero erosion, or the steady erosion rate of the soil given infinite exposure time (as is always true of a surface nuclide concentration without further information; see Lal, 1991). We then use equation (10) to calculate upper and lower bounds for  $R_{init}$  from these limiting values of the exposure time and the erosion rate. The result of this exercise, in which we find bounds for  $N_{10,exp}$  and then for  $R_{init}$ , is a range of possible values, that is, a probability distribution, for  $R_{init}$ . As we have calculated strict bounds for  $R_{init}$ , but these bounds were inferred from data subject to measurement error, this probability distribution is complicated. In practice, we facilitate error propagation by using a Gaussian probability distribution centered on the permitted range and with a standard deviation equal to half the permitted range. This probability distribution can then be propagated through equation (9) to calculate a new burial age and uncertainty, and the entire procedure can be iterated until it converges on a solution.

To summarize, it is not possible to obtain a unique value for  $R_{init}$ —all we can obtain is a probability distribution. This increases the uncertainty in the burial age. Fortunately, this uncertainty is small in our examples. In most landscapes, the erosion rate is fast enough—greater than a few meters per million years—that  $R_{init}$  is relatively insensitive to the erosion rate. In this study, we also benefit from the fact that exposure times of the paleosols are relatively short, on the order of hundreds of thousands of years in most cases. Figure 5 shows the estimates of  $R_{init}$  for the example paleosols in the Missouri till sequence. Even though the erosion rate and exposure time estimates have large uncertainties, they are in the region of figure 5 where these uncertainties result in only small uncertainties in  $R_{init}$ .

One additional refinement in estimating  $R_{init}$  is that we are dating a complete sequence of tills and paleosols, so we can estimate the exposure time for each paleosol. Knowing the exposure time means that an estimate of  $N_{10,exp}$  yields a unique value for the erosion rate and thence for  $R_{init}$ . We are still subject to the uncertainty in the inherited nuclide concentrations in this situation, but it narrows the range of possible  $R_{init}$  in some cases. Figure 5 shows this graphically. This reasoning is somewhat circular in that, when dating a particular till, we must a) use the ages of overlying tills to calculate the postdepositional nuclide production, and b) use the age of the underlying till to calculate the exposure time of the paleosol. That is, we would need to start with the uppermost till to calculate a) for all the tills, and we would need to start with the lowermost till to calculate b) for all the tills. In practice, the burial ages are only weakly sensitive to both of these effects, so we started with the uppermost till, calculated ages for the entire sequence of tills, and then repeated the calculations

using these first estimates of the burial age to compute the soil exposure times. This ensured an internally consistent set of age estimates.

Finally, there are two other complications in estimating  $R_{init}$ . First, paleosols beneath till are commonly truncated by subglacial erosion, so the surface of the preserved paleosol was not at the ground surface during exposure. This means that we must use the soil stratigraphy to estimate how much of the soil was truncated and take that into account in our estimate of the 'surface' production rate—that is, the production rate experienced by the uppermost sample—during exposure and soil formation that is needed to estimate  $R_{init}$  using equation (10). This contributes a very large uncertainty to the surface production rates used in this part of the calculation. For example, several of our example paleosols lacked an A horizon, but preserved a complete B horizon. Comparison to horizon thicknesses in complete soil profiles of similar age and topographic position suggests ~ 10 to 40 cm of truncation by subglacial erosion. This in turn implies a ~40 percent uncertainty in the surface production rate used in estimating  $R_{init}$ , which is much larger than the uncertainty in commonly accepted production rate calibrations (~10%; see Balco and others, 2008). Again, however (as discussed above and shown in fig. 5), this large uncertainty in the parameters used to estimate  $R_{init}$  has only a small effect on the overall burial age because of the insensitivity of  $R_{init}$  to these parameters in the range of interest.

Second, throughout the foregoing discussion we have assumed that the  $^{26}\text{Al}/^{10}\text{Be}$  production ratio is that for spallogenic production. The  $^{26}\text{Al}/^{10}\text{Be}$  production ratio is higher for production by muons (Heisinger and others, 2002a, 2002b). Thus, if a significant quantity of the  $^{26}\text{Al}$  and  $^{10}\text{Be}$  inventories produced during exposure and soil formation were produced by muon interactions, as would be the case for long exposure times at high erosion rates, or for samples collected deep below the paleosol surface, we would have to take this into account in estimating  $R_{init}$ . We did a series of numerical experiments to explore whether this effect would be important for the paleosols we describe here, and found that for the range of likely exposure times (~ 0.1–1 Myr), erosion rates (~ 10–20 m/Myr), and sample depths (mostly within 2.5 m of the paleosol surface) relevant to our sites, fully accounting for production by muons changes estimates of  $R_{init}$  by less than 1 percent. As this is well within the overall uncertainty of the calculation, we do not explicitly consider production by muons during soil formation and exposure (although, as discussed above, we do of course take it into account in calculating post-burial nuclide production). However, this issue is important at the Moberly paleosol in core WL3, where we analyzed samples that were several meters below the paleosol surface. At that depth, it would be important to account for production by muons in estimating  $R_{init}$ . We avoided this issue by excluding samples more than 2.5 m below the paleosol surface from the calculation of the isochron slope (although we did consider the deep samples in estimating the inherited nuclide concentrations).

#### *Complications Due To Varying Inheritance*

The assumption of constant inherited  $^{26}\text{Al}$  and  $^{10}\text{Be}$  in all the samples from a given paleosol—that is, that the soil parent material is homogeneous—is critical to this method. However, one of the advantages of this method, that it shares with any isochron method, is that whether or not the samples actually lie on an isochron provides a test of this assumption. If the samples were originally emplaced at the beginning of soil formation with significantly variable inherited  $^{26}\text{Al}$  and  $^{10}\text{Be}$  concentrations, the measured nuclide concentrations after exposure and burial could not lie on a straight line. This aspect of the isochron method is a significant improvement to the simple burial dating method in that whether or not the measurements lie on an isochron offers a test of some of the geologic assumptions needed to apply the method. This observation could be further quantified by applying statistical tests to compare the

scatter of the measurements around an isochron with their analytical uncertainty; we have not yet done this.

#### *Complete Algorithm*

The overall algorithm for calculating the burial age of a paleosol is therefore as follows:

1. Determine the slope of a line in  $^{26}\text{Al}$ - $^{10}\text{Be}$  space fit to the measurements. As the uncertainties in the  $^{26}\text{Al}$  and  $^{10}\text{Be}$  measurements are uncorrelated, the regression scheme of York (1966) can be used. Apply equation (9) to obtain an initial estimate for the burial age.
2. Using the initial burial age estimate, calculate the nuclide production in the samples after burial. As discussed above and further described in Balco and others (2005a), we use a 'sawtooth' age-depth model that includes steady surface erosion between the emplacement of the overlying units. Estimates of muon fluxes and interaction cross-sections are required in this step; we computed these using a MATLAB implementation, described in Balco and others (2008), of the method of Heisinger and others (2002a, 2002b).
3. Use the estimates for burial age and postdepositional production to correct the measured nuclide concentrations back to the time of burial. Estimate the inherited nuclide concentration and the range of possible values for  $R_{init}$ . Recalculate the age using this estimate of  $R_{init}$ . An estimate of the surface production rate is required in this step; we use the scaling scheme of Stone (2000) and the calibration data set from Balco and others (2008).
4. Repeat step 3 until the burial age converges to a solution.
5. Using the refined age derived in step 4, carry out steps 2–4 again. Repeat both inner and outer iteration loops until the burial age converges to a solution.

None of the examples in this paper required more than a few iteration loops.

Annotated MATLAB code that implements this algorithm appears as online supplementary data (<http://earth.geology.yale.edu/~ajs/SupplementaryData/2008/03BalcoMATLAB.tar>).

#### *Uncertainty Analysis*

The uncertainties in the burial age calculation include: i) measurement uncertainty, as expressed in the fit of an isochron to the measurements; ii) the uncertainty in estimating  $R_{init}$ , which is for the most part a function of how closely the measurements limit the inherited nuclide concentrations; iii) uncertainty in the  $^{26}\text{Al}$  and  $^{10}\text{Be}$  decay constants; iv) uncertainty in surface nuclide production rates, which is equivalent to the uncertainty in the truncation depth of the paleosol; and v) uncertainties in nuclide production rates after burial, which includes uncertainty in production rates due to muons as well as uncertainty in the ages, erosion rates, and bulk densities assumed for the overburden units.

We calculated the total uncertainties by assuming that the result is linear with respect to the input parameters, and adding in quadrature the product of the uncertainty in each of the input parameters and the partial derivative of the age with respect to that input parameter (for example, Bevington and Robinson, 1992). Expressions for the partial derivatives of the age with respect to the best-fit isochron slope, the decay constants, and  $R_{init}$  can be obtained from equation (9). We calculated the other partial derivatives—those with respect to the surface production rates, the age, density, and erosion rate of the overlying units, the age of the soil parent material, the truncation depth of the paleosol, and the production rates due to spallation and muons—numerically by a first-order centered difference approximation. This relatively simple method of uncertainty analysis is somewhat deficient in that it does not capture the asymmetry of the probability distribution for the age that results from

equation (9). However, a more elaborate uncertainty analysis—for example by Monte Carlo simulation—does not seem justified at present because approximating the age uncertainty by a normal distribution does not affect our geological conclusions. Table 4 shows the results of the uncertainty analysis. In addition, the MATLAB code in the online supplementary data includes detailed error diagnostics (<http://earth.geology.yale.edu/~ajs/SupplementaryData/2008/03BalcoMATLAB.tar>).

In all the examples in this paper, the overall uncertainty in the age is dominated by: i) the  $^{26}\text{Al}$  and  $^{10}\text{Be}$  measurement uncertainties, as expressed in the formal uncertainty of the best-fit isochron slope, and ii) the uncertainty in the decay constants. It follows from error analysis of equation (9) that: i) the uncertainty in fitting the isochron slope to the measurements is especially important at young ages: a 5 percent uncertainty in the isochron slope translates into a 50 percent age uncertainty for a 0.2 Ma paleosol, but only a 10 percent age uncertainty for a 1 Ma paleosol; and ii) given our typical measurement uncertainties, the uncertainty in the decay constants becomes more important than the uncertainty in the isochron slope for paleosols older than  $\sim 1.5$  Ma (fig. 6). These relationships are evident in our results (table 4): young ages have relatively large uncertainties that are dominated by the uncertainty in estimating the isochron slope; older ages have relatively smaller uncertainties, and uncertainties in the decay constants make a significant contribution. As we have discussed above, another important aspect of the error analysis is that all other uncertainties—that is, in surface and subsurface production rates, the amount of soil truncation by subglacial erosion, and the age-depth model for the overburden—are relatively unimportant in this study because the till immediately overlying the paleosols we sampled is always relatively thick. The greater the burial depth, the smaller the change in production rate with depth, so if the initial burial event is relatively deep, then even large uncertainties in the age, bulk density, and surface erosion rates of younger overburden units have a minor effect on the overall age estimate. Balco and others (2005c) made the same observation and provided a detailed uncertainty analysis. Even though the calculation method described here is different, a similar uncertainty analysis would closely duplicate the one already presented in that paper, so we have not repeated it here.

### *Sampling*

Several parts of the above discussion describe the effects of site selection and the choice of sample depth on the precision of the burial ages. This section summarizes these issues, as well as others not yet discussed, as a guide to applying the isochron method described above to buried paleosols in the field.

First, one important aspect of burial dating that we have not yet discussed is that most forms of burial dating rely on the sample remaining buried from the time of the initial burial event—the event that is to be dated—to the present. This is ensured by collecting samples from caves, boreholes, mine excavations, or very rapidly eroding (meters per year) bluffs or stream banks. In general, naturally exposed surface samples cannot be used for burial dating—re-exposure of the once-buried samples as they are brought to the surface by erosion violates the key assumptions of the method (although the application to river sediments discussed in the next section is a potential exception).

Second, this method relies on collecting a set of samples that have a wide range of  $^{10}\text{Be}$  and  $^{26}\text{Al}$  concentrations: to accurately determine the slope of the isochron, the range of nuclide concentrations among the samples must be significantly larger than the measurement uncertainties. This range of concentrations reflects the depth range over which the samples are collected, the relationship of the inherited nuclide concentrations in the paleosol parent material to the nuclide concentrations attributable to exposure during soil formation, and the depth and degree of soil mixing. If the

TABLE 4  
*Paleosol burial ages and uncertainties*

Paleosol	Overlying till	Site	Isochron slope	Burial age $t_b$ (Ma)	$\sigma t_b$ (Ma) ( $\sigma R_M$ only)	$\sigma t_b$ (Ma) (adding $\sigma R_{init}$ )	$\sigma t_b$ (Ma) (adding $\sigma \lambda_i$ )	$\sigma t_b$ (Ma) All uncertainties
-	-	3-B-99 core	$4.78 \pm 0.30$	0.69	0.13	0.13	0.14	0.14
Columbia	Macon	Sieger pit	$6.01 \pm 0.51$	0.22	0.18	0.18	0.18	0.18
Fulton	Columbia	PF2 core	$5.99 \pm 0.47$	0.22	0.17	0.17	0.17	0.17
Moberly	Fulton	WL3 core	$4.45 \pm 0.08$	0.82	0.04	0.04	0.08	0.08
Atlanta	Moberly	Musgrove pit	$3.66 \pm 0.52$	1.25	0.30	0.30	0.31	0.31
Atlanta <sup>1</sup>	Moberly	Musgrove pit	$3.69 \pm 0.02$	1.23	0.01	0.01	0.10	0.10

<sup>1</sup> After discarding sample MO-MP-04-250 as described in the text.

Note: The four different  $1 - \sigma$  uncertainties in the table show that different sources of uncertainty are important at different sites. These uncertainties take into account: i) the uncertainty in the isochron slope only; ii) the uncertainty in the isochron slope and the uncertainty in estimating the initial ratio  $R_{init}$ ; iii) the uncertainties in the isochron slope,  $R_{init}$ , and the  $^{29}\text{Al}$  and  $^{10}\text{Be}$  decay constants; and iv) all uncertainties, including those in nuclide production rates, our estimates of soil truncation depth, and the age, density, and erosion rate of overburden units. This highlights: i) the fact that the uncertainties derived from estimating  $R_{init}$  (estimating the soil truncation depth, and calculating the postdepositional nuclide concentration from the overburden age-depth model) are negligible in comparison to the measurement and decay constant uncertainties, and ii) the fact that measurement uncertainties are most important for young ages, and decay constant uncertainties are more important for older ages.

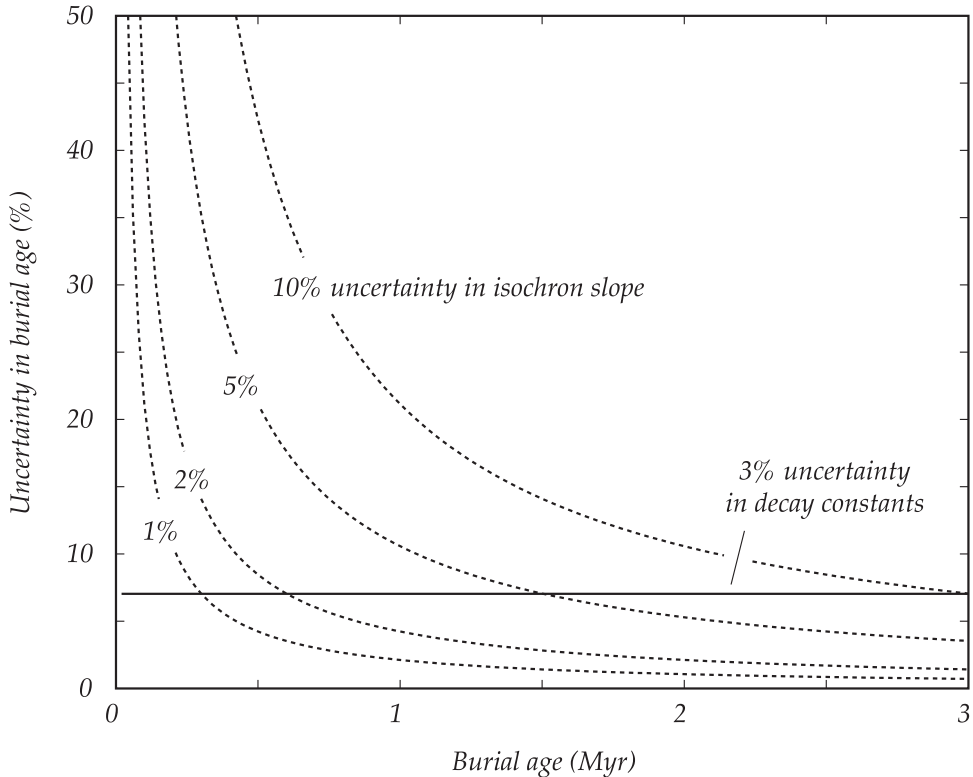


Fig. 6. Effect of measurement uncertainties and decay constant uncertainties on the precision of burial ages, derived from linear propagation of errors through equation (9). Each curve shows ( $1\sigma$ ) percentage uncertainty in the burial age ( $100 \times \sigma_{t_b}/t_b$ ) as a function of burial age. The dotted curves show the effect of uncertainties in the isochron slope derived from measurement uncertainties; the solid line shows the effect of the currently accepted uncertainty in  $^{26}\text{Al}$  and  $^{10}\text{Be}$  decay constants. A more precise measurement of the isochron slope reduces uncertainties in the burial age, but no matter how precise the slope determination, errors become large for relatively young burial ages. Uncertainty in the decay constants contributes a constant relative uncertainty no matter the burial age. The important point is that, given measurement uncertainties in this study, measurement uncertainty limits precision for young ages, and the decay constant uncertainty limits precision for old ages.

inherited nuclide concentration in the paleosol parent material is zero and there is no soil mixing, the  $^{10}\text{Be}$  concentrations in samples collected between the paleosol surface and 1 meter below it would vary by a factor of  $\sim 4$ , which would yield a relatively precise isochron slope. Nuclide inheritance and soil mixing both act to reduce the range of nuclide concentrations for a given range of sample depths. This is evident from the results of this study: the range of sample depths at our sites was 2 to 10 m, but in some cases the measured  $^{10}\text{Be}$  concentrations only varied by a factor of 2. Sampling over a wider depth range would increase the range of nuclide concentrations and, as noted above, would improve the estimate of  $R_{init}$  by better constraining inherited nuclide concentrations. However, as also noted above, sampling more than  $\sim 2$  to 2.5 m below the paleosol surface increases the importance of production by muons during soil formation, potentially degrading the estimate of  $R_{init}$ . In principle, logarithmically spaced samples would yield evenly spaced nuclide concentrations and thus a better-behaved determination of the isochron slope, but soil mixing processes mean that this is unlikely to work in practice. It seems that the most practical approach is to collect several evenly spaced samples between the paleosol surface and  $\sim 1.5$  to 2 m below it.



Third, the discussion above emphasizes that uncertainties in the burial history of the paleosol have a small effect on the overall precision of the burial age only if the till immediately overlying the paleosol is relatively thick. This is true because the change in nuclide production rates with depth becomes smaller as the depth increases. Even if we know nothing about the geologic history of the site after the emplacement of the till immediately overlying a paleosol, we know that the paleosol has always been shielded by at least the thickness of this first till. If the first till is thick, then even very large subsequent changes in the burial depth of the paleosol have only a small effect on post-burial production. Exactly how thick is thick enough for this condition to be true depends on the inherited nuclide concentrations, the nuclide concentrations attributable to exposure during soil formation, the duration of burial, and the measurement uncertainties (see Balco and others, 2005b, 2005c; Blard and others, 2006, for more information). Many of these factors cannot be determined in advance of sampling, so the thickness of the overlying till required to maintain a certain precision in the burial age can only be accurately computed *ex post facto*. In practice, given current measurement uncertainties, Pleistocene burial ages, and the present understanding of nuclide production by muons, the till immediately overlying the paleosol should be several meters thick. In this study, we sampled only sites where the till immediately overlying the paleosol was at least 5 m ( $\sim 1000 \text{ g cm}^{-2}$ ) thick.

#### DATA REDUCTION METHODS III: OTHER STRATIGRAPHIC SITUATIONS

The preceding section developed a specific application of the  $^{26}\text{Al}$ - $^{10}\text{Be}$  burial isochron method to till-paleosol sequences; in this section we describe another possible variant to show how the general approach could be applied in a wider range of geologic situations. Discussions with D. Granger, who brought the following example to our attention, contributed to this section. The important features of till-paleosol sequences that we used in constructing the method above are: i) the tills in which the paleosols are formed contain significant, well-mixed, and unknown amounts of inherited  $^{26}\text{Al}$  and  $^{10}\text{Be}$ ; ii) the tills immediately overlying the paleosols are thick enough that uncertainties in post-burial nuclide production have an insignificant effect on the burial age, that is, post-burial production can be considered a known quantity rather than an additional unknown parameter; and iii) soil-forming processes and subglacial deformation preclude any assumptions about the time-depth history of the samples prior to burial. These features of the geologic situation guided our mathematical approach, in which we derived a relationship between the nuclide concentrations and the burial age that did not depend on the sample depth or the inherited nuclide concentrations. In fact, this is only one possible isochron method for burial dating, and there are other geologic situations, leading to different sets of assumptions, that could be addressed with similar isochron methods.

For example, several previous studies (for example, Granger and Smith, 2000) have used the simple burial dating approach to date fluvial sediments preserved in river terraces. Sediments that originate from steady erosion of a basin and then are buried in a fill terrace have experienced only a two-stage exposure history, satisfying the main assumption of the simple burial dating approach. However, river terrace sediments are commonly relatively thin, so post-burial nuclide production is a significant part, even the majority, of the measured nuclide inventory. Thus, the simple burial age is very sensitive to uncertainties in the post-burial production derived from both uncertainties in subsurface nuclide production rates and uncertainties in the depositional or erosional history of the terrace surface. In this case, we need a method that allows the burial age of the sediment to be determined without any knowledge of the post-burial nuclide production. This can be accomplished by measuring  $^{26}\text{Al}$  and  $^{10}\text{Be}$  concentrations in a range of individual clasts collected from the same stratigraphic level in the terrace sediment. Several past studies have established that



cosmogenic-nuclide concentrations in individual clasts from a sample of river sediment vary widely; nuclide concentrations in a given clast as well as in the aggregate of all clasts are in equilibrium with steady erosion, but the samples originate from locations in the watershed that are subject to different nuclide production rates and surface erosion rates (Brown and others, 1995; Repka and others, 1997; Codilean and others, 2008). However, post-burial nuclide production will be the same in clasts that are collected at the same stratigraphic level. In this scenario, given the assumptions that i) nuclide production during erosion is by spallation only, and ii) the erosion rate in the watershed is rapid enough that radioactive decay can be disregarded, the  $^{26}\text{Al}$  and  $^{10}\text{Be}$  concentrations measured in a clast at the present time are:

$$N_{10,m} = \frac{P_{10}(0)\Lambda}{\varepsilon} e^{-t\lambda_{10}} + N_{10,pb} \quad (11)$$

$$N_{26,m} = \frac{P_{26}(0)\Lambda}{\varepsilon} e^{-t\lambda_{26}} + N_{26,pb} \quad (12)$$

where  $\varepsilon$  is the erosion rate ( $\text{g cm}^{-2} \text{yr}^{-1}$ ) where the clast originated, and  $N_{26,pb}$  and  $N_{10,pb}$  are the post-burial  $^{26}\text{Al}$  and  $^{10}\text{Be}$  concentrations (atoms  $\text{g}^{-1}$ ) in any clast collected from the same stratigraphic level. As we do not know the upstream erosion rate for any particular clast, we can follow a similar approach to the previous section and eliminate  $\varepsilon$  by solving equation (11) for  $\Lambda/\varepsilon$ , and substituting into equation (12). This yields a relationship between the measured  $^{26}\text{Al}$  and  $^{10}\text{Be}$  concentrations in a set of clasts:

$$N_{26,m} = \frac{P_{26}(0)}{P_{10}(0)} e^{-(\lambda_{26}-\lambda_{10})t_b} N_{10,m} - \frac{P_{26}(0)}{P_{10}(0)} e^{-(\lambda_{26}-\lambda_{10})t_b} N_{10,pb} + N_{26,pb} \quad (13)$$

Again, equation (13) is a linear relation between the measured  $^{26}\text{Al}$  and  $^{10}\text{Be}$  concentrations that is true regardless of the erosion rate where the clast originated. The slope of this line is the same as the slope of the line defined by equation (8). It depends on the  $^{26}\text{Al}/^{10}\text{Be}$  production ratio, the  $^{26}\text{Al}$  and  $^{10}\text{Be}$  decay constants, and the burial time, but not on the post-burial production. Thus, we could analyze a set of clasts from the same depth in a river terrace and, if the clasts had originated from sites with a wide enough range of erosion rates, we could fit a line to the  $^{26}\text{Al}$  and  $^{10}\text{Be}$  concentrations and determine a burial age for the terrace that did not depend on any assumptions about subsurface nuclide production rates or the time-depth history of the samples after they were originally buried. To summarize, the different geologic histories of the till-paleosol sequences discussed in the preceding section and the river terrace sediments discussed in this section lead to different sets of known and unknown parameters. In both cases, the approach of collecting samples that share the same burial age, but whose exposure histories differ in one of the other unknown parameters, leads to an isochron method that can be used to infer the burial age of the samples independently of the unknowns. We expect that similar approaches can be used in a variety of geologic situations.

#### RESULTS AND DISCUSSION

In this section, we apply the  $^{26}\text{Al}$ - $^{10}\text{Be}$  isochron method for till-paleosol sequences that we described above to examples from glacial sediment sequences in the north-central US. First, we apply it to a paleosol in the 3-B-99 borehole in eastern Nebraska that has already been dated by Balco and others (2005c). As described above, in this previous paper we calculated an  $^{26}\text{Al}$ - $^{10}\text{Be}$  burial age for the paleosol by inversion of a forward model calculation of the  $^{26}\text{Al}$  and  $^{10}\text{Be}$  concentrations at specific depths in the

paleosol; here we establish consistency between the two approaches by showing that the isochron method yields the same burial age without the requirement of modeling the time-depth history of the samples during soil formation. Second, we use the isochron method to date the complete sequence of tills and intercalated paleosols in central Missouri, described in the introduction, whose ages are not yet known.

#### *Application To Existing Data, Eastern Nebraska*

In the 3-B-99 borehole in eastern Nebraska, a paleosol is developed in till and buried by a sequence of three loess units, the upper two of which have been independently dated; thus the goal of Balco and others (2005c) was to date the lowest loess by  $^{26}\text{Al}$ - $^{10}\text{Be}$  burial dating of the paleosol. The paleosol has a complete A horizon, and the unit immediately overlying it is not till but loess; thus the paleosol was not truncated at burial. The ages, thicknesses, and densities of the overlying units are reported in Balco and others (2005c) and in the MATLAB code (<http://earth.geology.yale.edu/~ajs/SupplementaryData/2008/03BalcoMATLAB.tar>). The  $^{26}\text{Al}$  and  $^{10}\text{Be}$  concentrations, as predicted by equation (8), define an isochron with a slope less than the production ratio (fig. 7). The isochron method yields an age for the lowermost loess unit of  $0.69 \pm 0.14$  Ma, which is similar to the age of  $0.65 \pm 0.14$  Ma obtained from the same data using the forward model approach [the result of the forward model approach stated here differs from the value of  $0.58 \pm 0.12$  stated in Balco and others (2005c) because the  $^{10}\text{Be}$  concentrations and decay constants in that paper were referenced to the Be standards of Nishiizumi (2002), whereas in this paper we have adopted those of Nishiizumi and others (2007) as discussed above]. In addition to a burial age, the forward modeling method yielded estimates of the inherited  $^{26}\text{Al}$  and  $^{10}\text{Be}$  concentrations. These lie on the isochron defined by the data, as expected from equation (8), indicating consistency between the two approaches (fig. 7). The small difference in the central age estimate results from the choice of the fitting parameter used in the forward model approach: the forward model optimization method seeks to fit the actual  $^{26}\text{Al}$  and  $^{10}\text{Be}$  concentrations at specific depths in the soil rather than the slope of the data in  $^{26}\text{Al}$ - $^{10}\text{Be}$  space. It is not clear which approach ought to be more accurate. We suggest that, even though the forward model is a good fit to the data in this example, the isochron method is still preferred because it does not rely on the assumption that the samples remained at a constant depth during exposure and soil formation.

#### *New Measurements from Missouri Paleosols*

*Columbia paleosol, Sieger pit.*—This paleosol is developed in the Columbia till and overlain by the Macon till, so its burial age gives the age the Macon till was emplaced. A 5-cm-thick A horizon was present, and the soil appeared otherwise undisturbed. At this site and at the others discussed below, we estimated the thickness of the soil profile removed by subglacial erosion by comparing soil horizon thicknesses to those in stratigraphically equivalent paleosols at other sites. Soil horizon thickness can vary significantly with the topographic position, surface erosion rate, and hydrology of a site; we accounted for this variation by assigning a 100 percent uncertainty to our estimate of the truncation depth. As discussed above, even a large uncertainty in this parameter contributes only a small uncertainty to the burial age; the results in table 4 show this as well. At this site, stratigraphically equivalent paleosols in nearby sections have A horizon thicknesses between 0 and 30 cm, so we assumed a truncation depth of  $20 \pm 20$  cm in the age calculation. The paleosol at this site is overlain by the Macon till as well as by thin loess (table 2). As we are treating only the age of the Macon till as an unknown, we assumed (at this site and at others where the loess is present) that the loess was deposited  $125 \pm 50$  ka for purposes of calculating the post-burial production.

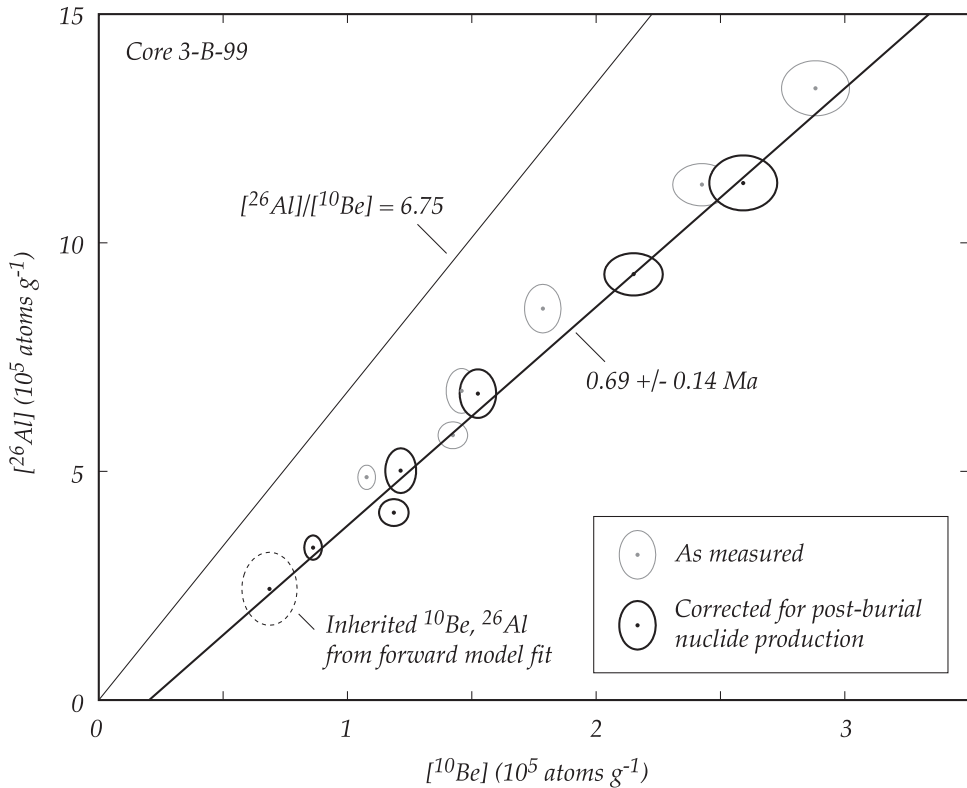


Fig. 7. Isochron method applied to the paleosol in borehole 3-B-99 in eastern Nebraska described in Balco and others (2005c). In this and subsequent figures, the light gray ellipses are 68% confidence ellipses for the raw  $^{26}\text{Al}$  and  $^{10}\text{Be}$  measurements on paleosol quartz. The black ellipses reflect correction of the measured data to remove nuclide production after burial, as described in the text. The dark line is the isochron that best fits the corrected data, from which we infer the burial age of the paleosol. The light line has a slope given by the production ratio  $P_{26}(0)/P_{10}(0)$  for comparison. In this figure only, the dotted ellipse shows the inherited  $^{26}\text{Al}$  and  $^{10}\text{Be}$  concentrations calculated (independently of the isochron method) by forward model optimization in Balco and others (2005c). These lie on the isochron, indicating consistency between the two methods.

Nuclide concentrations at this site decrease with depth below the soil surface for the most part, suggesting limited vertical mixing during soil formation (fig. 2). However, near the surface both  $^{26}\text{Al}$  and  $^{10}\text{Be}$  concentrations decreased with depth more steeply than expected for spallogenic production, suggesting vertical strain or soil deflation. Regardless, the data define an isochron that yields a burial age for the paleosol—that is, a depositional age for the Macon till—of  $0.22 \pm 0.18 \text{ Ma}$  (fig. 8). The large relative uncertainty, as discussed above, results from the property of equation (9) that uncertainties in the isochron slope result in proportionally larger age uncertainties at younger ages (fig. 6). Other uncertainties in the input parameters have a negligible effect on the overall uncertainty (table 4).

The only existing age constraints on the Macon till are that it is normally magnetized, so must be younger than 0.78 Ma (Rovey and Tandarich, 2006), and that it is older than the Stage 7 interglaciation near 0.2 Ma (Rovey, 1997). Our new age estimate is consistent with these constraints.

*Fulton paleosol, PF2 borehole.*—This paleosol is developed in the Fulton till and overlain by the Columbia till, so its burial age gives the age the Columbia till was

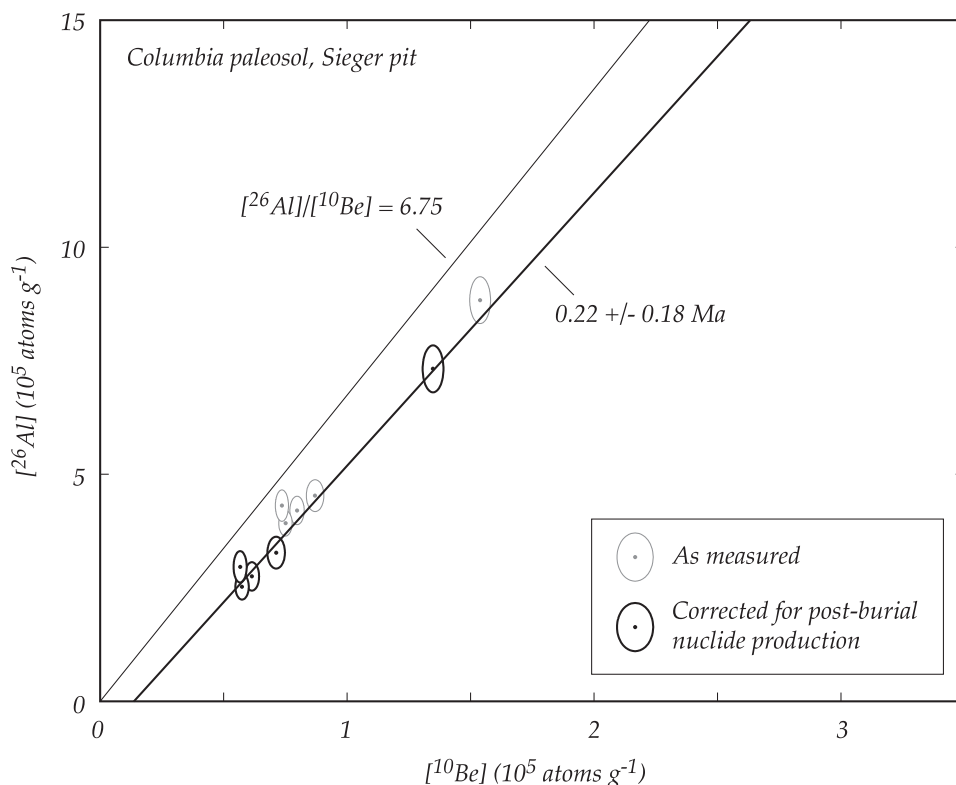


Fig. 8. Isochron method applied to the Columbia paleosol at the Sieger pit. This site yields the age of the overlying Macon till. The symbols are as described in figure 7.

emplaced. No A horizon was present in this paleosol in either this core or in an adjacent core collected several meters away. The B horizon was 2.3 m thick in both cores, in agreement with B horizon thicknesses for stratigraphically equivalent paleosols elsewhere. However, in this core, there were obvious shear planes in the upper 2 m of the paleosol, and grain size and clay mineralogy were nearly constant throughout the B horizon, in contrast to equivalent paleosols at other sites that characteristically show gradational changes in these parameters through the B horizon. These observations suggest that this paleosol was mixed, down to the bottom of the B horizon, by subglacial deformation. This is consistent with the observation that our uppermost three samples in this paleosol, which were all in the B horizon, had indistinguishable  $^{26}\text{Al}$  and  $^{10}\text{Be}$  concentrations (fig. 2). Below the B horizon, a normal weathering sequence—a leached zone with oxidized mottles grading downward into an oxidized zone with gleyed mottles—is present, and nuclide concentrations decrease. Thus, it appears that the entire A horizon was removed by subglacial erosion, and the B horizon was mixed by subglacial deformation. We accounted for this by assuming a truncation depth of  $30 \pm 30$  cm in the age calculation.

Furthermore, we were not able to collect an undisturbed core through this paleosol. For the upper two samples (PF2-45.75-48 and PF2-48.75-52) we had only ~ 50 percent recovery within each cored interval, and were not able to determine what part of the interval we recovered.

Despite the severe disturbance of this paleosol, the  $^{26}\text{Al}$  and  $^{10}\text{Be}$  measurements define an isochron (fig. 9). The upper three samples in this soil had similar nuclide

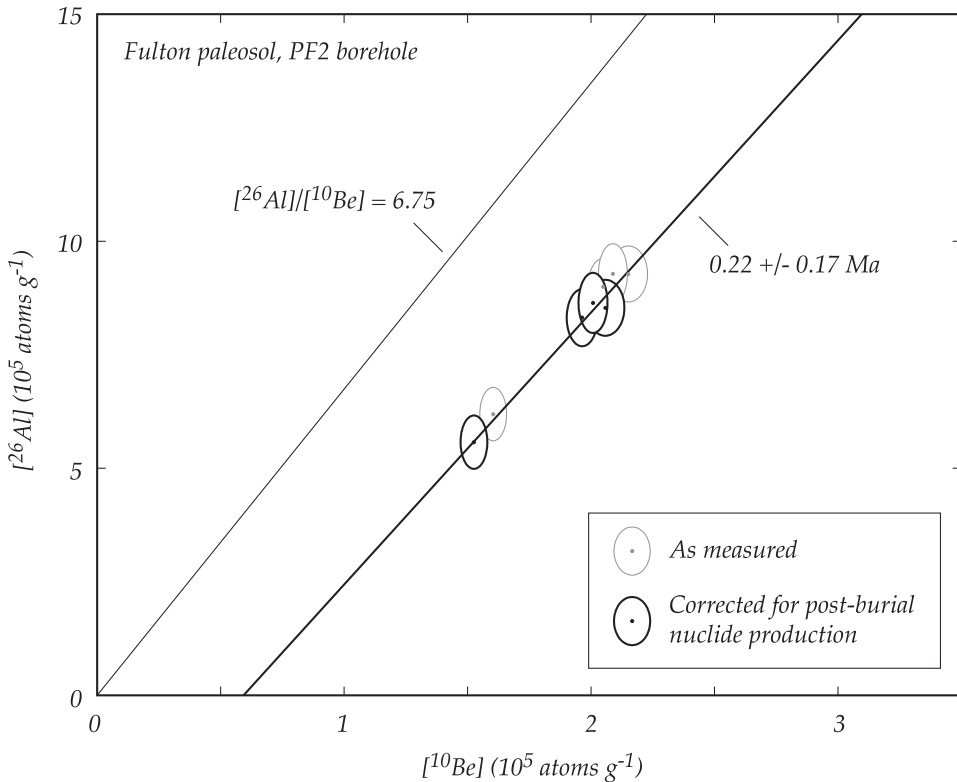


Fig. 9. Isochron method applied to the Fulton paleosol in the PF2 borehole. This site yields the age of the overlying Columbia till. The symbols are as described in figure 7.

concentrations, so the isochron is essentially defined by only two points. This makes it impossible to evaluate the assumption that inherited nuclide concentrations were constant at all depths. The isochron yields an age of  $0.22 \pm 0.17 \text{ Ma}$  for the Columbia till. The large uncertainty is again the result of a relatively large uncertainty in the slope of the isochron combined with a relatively young age.

The only independent age constraints on the Columbia till are that it is normally magnetized and that it must predate the Macon till and postdate the Fulton till. Our age estimate is consistent with these constraints. An important point here, however, is that the Columbia is stratigraphically lower than the Macon, so if the age estimates for these tills overlap, they cannot be considered independently. The two age estimates, considered individually, imply a finite probability that, for example, the Macon till could date to  $0.3 \text{ Ma}$  and the Columbia till could date to  $0.2 \text{ Ma}$ . In reality, the fact that the Macon overlies the Columbia means that the probability of this outcome is zero. Thus, the stratigraphic relationship between the two tills provides an additional constraint that limits the probability distribution for each age. Several authors (for example, Muzikar and Granger, 2006, and references therein) give analytical approaches to this problem; we used a Monte Carlo simulation where we sampled the independent age estimates, and discarded samples that did not satisfy the constraints that: i) the Macon must be younger than the Columbia, and ii) each age must be greater than zero. Resulting age estimates that take account of these constraints are  $0.17 \pm 0.11 \text{ Ma}$  for the Macon till and  $0.33 \pm 0.13 \text{ Ma}$  for the Columbia till. Taken with

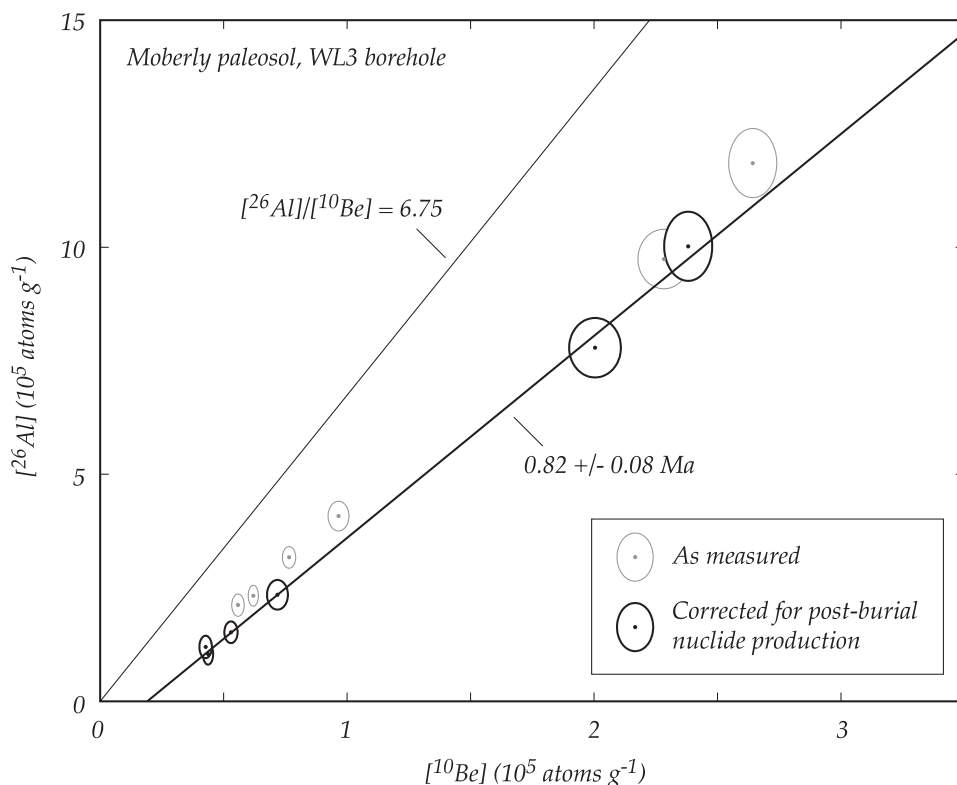


Fig. 10. Isochron method applied to the Moberly paleosol in the WL3 borehole. This site yields the age of the overlying Fulton till. The symbols are as described in figure 7.

the observation that the Macon till must be older than Stage 7 (Rovey, 1997), these results suggest a Stage 8 ( $\sim 0.25$  Ma) age for the Macon till and a Stage 10 ( $\sim 0.35$  Ma) or Stage 12 ( $\sim 0.45$  Ma) age for the Columbia till. However, with these data we cannot exclude the possibility that the Macon and Columbia tills record closely spaced ice sheet advances during only one of these major glaciations.

*Moberly paleosol, WL3 borehole.*—This paleosol is developed in the Moberly till and overlain by the Fulton till, so its burial age gives the age the Fulton till was emplaced. An E horizon is preserved, suggesting little subglacial erosion during the emplacement of the overlying till. We assumed a truncation depth of  $20 \pm 20$  cm. Nuclide concentrations increased with depth in the upper 1 m of the paleosol before decreasing, suggesting significant vertical mixing in this layer during soil formation. As discussed above, we did not use the two deepest samples from this paleosol (table 3) in calculating the isochron slope to avoid complications in estimating  $R_{mit}$  caused by nuclide production due to muons.

This paleosol yielded an age of  $0.82 \pm 0.07$  for the Fulton till (fig. 10). The uncertainty is significantly smaller for this till than for the younger tills discussed above because i) a wider range in the measured nuclide concentrations reduced uncertainty in the slope of the isochron, and ii) the fact that this burial age is older reduces the importance of the slope uncertainty on the relative age uncertainty. In this case a significant amount of the total uncertainty is contributed by the uncertainty in the  $^{26}\text{Al}$  and  $^{10}\text{Be}$  decay constants (table 4 and fig. 6).

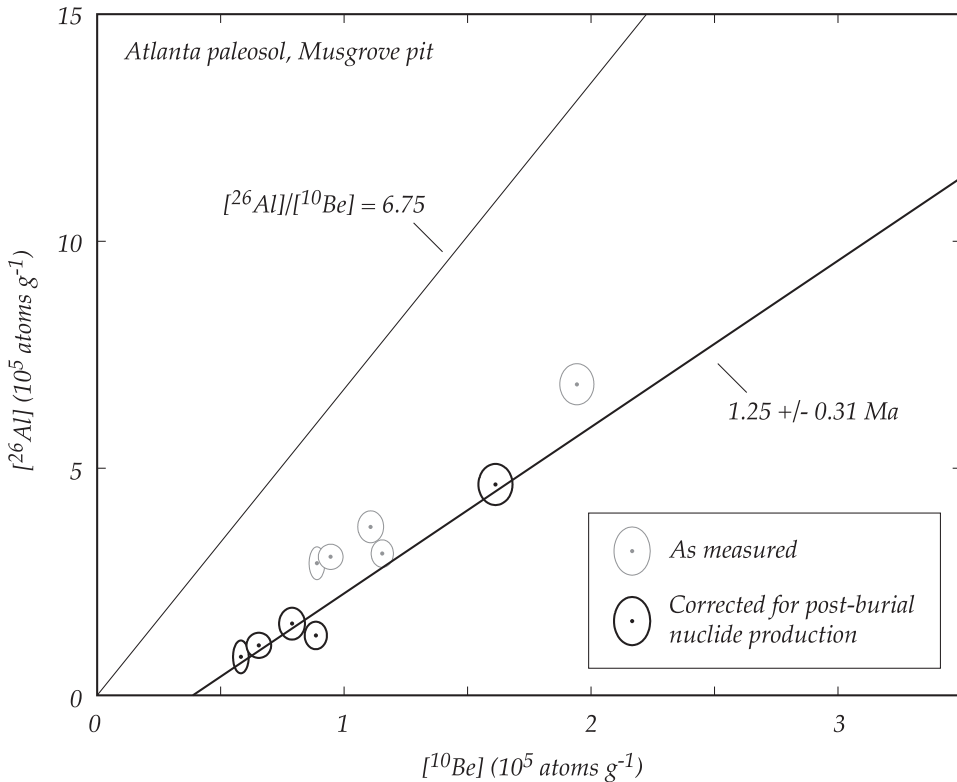


Fig. 11. Isochron method applied to the Atlanta paleosol at the Musgrove pit. This site yields the age of the overlying Moberly till. The symbols are as described in figure 7.

The Fulton till is normally magnetized, so must be younger than 0.78 Ma. Our age estimate is consistent with this constraint and, in fact, appears to closely limit the age of the till to near 0.78 Ma.

*Atlanta paleosol, Musgrove pit.*—This paleosol is developed in the Atlanta till and overlain by the Moberly till, so its burial age gives the age the Moberly till was emplaced. An A horizon is present, as well as flattened twigs and organic debris at the contact between the paleosol and the overlying Moberly till. This indicates that the paleosol was not truncated during burial. As at the Sieger Pit, nuclide concentrations generally decrease with depth but do so more rapidly than expected from the depth-dependence of spallogenic production, again suggesting vertical strain or deflation during soil formation.

This paleosol yielded an age of  $1.25 \pm 0.31 \text{ Ma}$  for the Moberly till (fig. 11). The uncertainty is dominated by the uncertainty in the isochron slope (table 4). In this case, however, most of the uncertainty in the isochron slope is the result of a single measurement (fig. 11; sample MO-MP-04-250 in table 3); if this sample were excluded the age would be  $1.23 \pm 0.10 \text{ Ma}$ , and the decay constant uncertainty would become an important part of the total uncertainty.

The Moberly till and associated sediments are reversely magnetized, suggesting deposition prior to 0.78 Ma (Rovey and Tandarich, 2006; Rovey and others, 2006). Balco and others (2005a) also estimated the age of the Moberly till from the simple burial age of a single sample collected at the Musgrove pit: this yielded a maximum limiting age of 1.8 Ma. Our new age estimate agrees with these constraints.



## SUMMARY AND CONCLUSIONS

We have described a method for measuring the burial age of paleosols in till-paleosol sequences that is based on the idea that the  $^{26}\text{Al}$  and  $^{10}\text{Be}$  concentrations of quartz samples collected from a range of depths below the paleosol surface will lie on an isochron. The only critical assumption required by this method is that the inherited  $^{26}\text{Al}$  and  $^{10}\text{Be}$  concentrations in the paleosol parent material are well-mixed vertically. An important advantage of this method relative to other approaches to burial dating is that this assumption can be tested by observation of whether the measured  $^{26}\text{Al}$  and  $^{10}\text{Be}$  concentrations do in fact define a linear isochron, and the assumption appears to hold for the paleosols we describe in this study.

Applying this method to a sequence of intercalated tills and paleosols in central Missouri yields ages for the tills that are correctly stratigraphically ordered as well as consistent with paleomagnetic age constraints. In previous work, we dated the oldest till in the Missouri sequence to  $\sim 2.5$  Ma; here we show that ice sheet advances also occurred near 1.25 Ma, 0.8 Ma, and twice near 0.4 to 0.2 Ma. Our goal in future research is to further validate the method by dating the same tills at different field sites. We will discuss these efforts as well as the overall significance of the chronology of ice sheet advances in a future paper.

A previously described method for burial dating of paleosols that contain inherited  $^{26}\text{Al}$  and  $^{10}\text{Be}$  used a forward model optimization approach to determine not only the burial age of the paleosol, but also the inherited nuclide concentrations and information about the exposure time and erosion rate of the paleosol prior to burial. The new isochron method explicitly determines only the burial age, and, because it discards information that could potentially be gained from the depth-nuclide concentration profile in the paleosol, is subject to irreducible uncertainties that limit the precision of the burial age in some situations. However, the accuracy of the forward-modeling approach is critically dependent on the assumption that neither i) soil-forming processes that cause vertical mixing or strain, or ii) disturbance of the soil stratigraphy either by subglacial deformation during burial or during core recovery, are important. In practice, these processes are nearly always important, and the fact that the new isochron method requires no assumptions about the age-depth history of the samples during soil formation means that it can be applied in more general stratigraphic settings. Furthermore, the overall idea of forming an  $^{26}\text{Al}$ - $^{10}\text{Be}$  isochron from a set of samples that share the same burial age, but whose exposure histories differ in other ways, is more general than the application to till-paleosol sequences that we have discussed here. It can be used to construct similar multiple-cosmogenic-nuclide isochron methods applicable in different geologic settings.

## ACKNOWLEDGMENTS

The majority of this work was supported by NSF award EAR-0545023. A research grant from the Prairie Fork Trust supported analyses of core PF2. Pat Jones, Reggie Bennett, Jamie and Debbie Coe, and Eagle Scout Joseph Bucheit and his Boy Scout troop, as well as others at the Missouri Department of Transportation, the Missouri Department of Conservation, the National Resource Conservation Service, the Missouri Association of Professional Soil Scientists, and the University of Missouri, all helped to make this funding and the drilling at Prairie Fork possible. In addition, we thank Mike Siemens at the Missouri Geological Survey, Jeff Porter at Christy Minerals, and Ray Nordwald at Harbison-Walker Refractories Company for providing access to archived drill core and active clay mining operations. This manuscript was reviewed by D. Granger, P.-H. Blard, and R. Heermance; we particularly appreciate P.-H. Blard's careful attention to the mathematics and D. Granger's calling our attention to the river sediment example.

## REFERENCES

- Anderson, R. S., Repka, J. L., and Dick, G. S., 1996, Explicit treatment of inheritance in dating depositional surfaces using *in situ*  $^{10}\text{Be}$  and  $^{26}\text{Al}$ : *Geology*, v. 24, p. 47–51, doi:10.1130/0091-7613(1996)024<0047:ETOIID>2.3.CO;2.
- Balco, G., Rovey, C. W., II, and Stone, J. O. H., 2005a, The first glacial maximum in North America: *Science*, v. 307, p. 222, doi:10.1126/science.1103406.
- Balco, G., Stone, J. O. H., and Jennings, C., 2005b, Dating Plio-Pleistocene glacial sediments using the cosmic-ray-produced radionuclides  $^{10}\text{Be}$  and  $^{26}\text{Al}$ : *American Journal of Science*, v. 305, p. 1–41, doi:10.2475/ajs.305.1.1.
- Balco, G., Stone, J. O. H., and Mason, J. A., 2005c, Numerical ages for Plio-Pleistocene glacial sediment sequences by  $^{26}\text{Al}/^{10}\text{Be}$  dating of quartz in buried paleosols: *Earth and Planetary Science Letters*, v. 232, p. 179–191, doi:10.1016/j.epsl.2004.12.013.
- Balco, G., Stone, J., Lifton, N., and Dunai, T., 2008, A complete and easily accessible means of calculating surface exposure ages or erosion rates from  $^{10}\text{Be}$  and  $^{26}\text{Al}$  measurements: *Quaternary Geochronology*, v. 3, p. 174–195, doi:10.1016/j.quageo.2007.12.001.
- Bevington, P., and Robinson, D. K., 1992, *Data Reduction and Error Analysis for the Physical Sciences*: Boston, WCB McGraw-Hill, 328 p.
- Blard, P.-H., Bourlès, D., Lavé, J., and Pik, R., 2006, Applications of ancient cosmic-ray exposures: Theory, techniques, and limitations: *Quaternary Geochronology*, v. 1, p. 59–73, doi:10.1016/j.quageo.2006.06.003.
- Brown, E. T., Stallard, R. F., Larsen, M. C., Raisbeck, G. M., and Yiou, F., 1995, Denudation rates determined from the accumulation of *in-situ*-produced  $^{10}\text{Be}$  in the Luquillo Experimental Forest, Puerto Rico: *Earth and Planetary Science Letters*, v. 129, p. 193–202, doi:10.1016/0012-821X(94)00249-X.
- Codilean, A. T., Bishop, P., Stuart, F. M., Hoey, T. B., Fabel, D., and Freeman, S.P.H.T., 2008, Single-grain cosmogenic  $^{21}\text{Ne}$  concentrations in fluvial sediments reveal spatially variable erosion rates: *Geology*, v. 36, p. 159–162, doi:10.1130/G24360A.1.
- Emiliani, C., 1955, Pleistocene temperatures: *Journal of Geology*, v. 63, p. 538–578.
- Granger, D., 2006, A review of burial dating methods using  $^{26}\text{Al}$  and  $^{10}\text{Be}$ , *in* Siame, L. L., Bourlès, D. L., and Brown, E. T., editors, *In-situ*-produced cosmogenic nuclides and quantification of geological processes: Geological Society of America Special Paper 415, p. 1–16, doi: 10.1130/2006.2415(01).
- Granger, D. E., and Smith, A. L., 2000, Dating buried sediments using radioactive decay and muogenic production of  $^{26}\text{Al}$  and  $^{10}\text{Be}$ : *Nuclear Instruments and Methods in Physics Research B*, v. 172, p. 822–826, doi:10.1016/S0168-583X(00)00087-2.
- Heisinger, B., Lal, D., Jull, A. J. T., Kubik, P., Ivy-Ochs, S., Neumaier, S., Knie, K., Lazarev, V., and Nolte, E., 2002a, Production of selected cosmogenic radionuclides by muons 1. Fast muons: *Earth and Planetary Science Letters*, v. 200, p. 345–355, doi:10.1016/S0012-821X(02)00640-4.
- Heisinger, B., Lal, D., Jull, A. J. T., Kubik, P., Ivy-Ochs, S., Knie, K., and Nolte, E., 2002b, Production of selected cosmogenic radionuclides by muons: 2. Capture of negative muons: *Earth and Planetary Science Letters*, v. 200, p. 357–369, doi:10.1016/S0012-821X(02)00641-6.
- Lal, D., 1991, Cosmic ray labeling of erosion surfaces: *in situ* nuclide production rates and erosion models: *Earth and Planetary Science Letters*, v. 104, p. 424–439, doi:10.1016/0012-821X(91)90220-C.
- Lal, D., and Chen, J., 2005, Cosmic ray labeling of erosion surfaces II: Special cases of exposure histories of boulders, soil, and beach terraces: *Earth and Planetary Science Letters*, v. 236, p. 797–813, doi:10.1016/j.epsl.2005.05.025.
- Muzikar, P., and Granger, D., 2006, Combining cosmogenic, stratigraphic, and paleomagnetic information using a Bayesian approach: General results and an application to Sterkfontein: *Earth and Planetary Science Letters*, v. 243, p. 400–408, doi:10.1016/j.epsl.2005.12.020.
- Nishiizumi, K., 2002,  $^{10}\text{Be}$ ,  $^{26}\text{Al}$ ,  $^{36}\text{Cl}$ , and  $^{41}\text{Ca}$  AMS standards: Nagoya, Japan, Nagoya University, 9th Conference on Accelerator Mass Spectrometry, Abstract 016-1, p. 130.
- 2004, Preparation of  $^{26}\text{Al}$  AMS standards: *Nuclear Instruments and Methods in Physics Research B*, v. 223-224, p. 388–392, doi:10.1016/j.nimb.2004.04.075.
- Nishiizumi, K., Winterer, E. L., Kohl, C. P., Klein, J., Middleton, R., Lal, D., and Arnold, J. R., 1989, Cosmic Ray Production Rates of  $^{10}\text{Be}$  and  $^{26}\text{Al}$  in Quartz From Glacially Polished Rocks: *Journal of Geophysical Research*, v. 94, p. 17,907–17,915, doi:10.1029/JB094iB12p17907.
- Nishiizumi, K., Imamura, M., Caffee, M. W., Southon, J. R., Finkel, R. C., and McAninch, J., 2007, Absolute calibration of  $^{10}\text{Be}$  AMS standards: *Nuclear Instruments and Methods in Physics Research B*, v. 258, p. 403–413, doi:10.1016/j.nimb.2007.01.297.
- Repka, J., Anderson, R., and Finkel, R., 1997, Cosmogenic dating of fluvial terraces, Fremont River, Utah: *Earth and Planetary Science Letters*, v. 152, p. 59–73, doi:10.1016/S0012-821X(97)00149-0.
- Rovey, C. W., II, 1997, The nature and origin of gleyed polygenetic paleosols in the loess covered glacial drift plain of Northern Missouri, USA: *Catena*, v. 31, p. 153–172, doi:10.1016/S0341-8162(97)00037-4.
- Rovey, C. W., II, and Kean, W. F., 1996, Pre-Illinoian Glacial Stratigraphy in North-Central Missouri: *Quaternary Research*, v. 45, p. 17–29, doi:10.1006/qres.1996.0002.
- Rovey, C. W., II, and Tandarich, J., 2006, Lithostratigraphy of Glacigenic Sediments in North-Central Missouri, *in* Mandel, R., editor, *Guidebook of the 18th Biennial Meeting of the American Quaternary Association: Kansas Geological Survey Technical Series 21*, p. 3–A–1—3–A–12.
- Rovey, C. W., II, Kean, W., and Atkinson, L., 2006, Paleomagnetism of sediments associated with the Atlanta Formation, north-central Missouri, USA, *in* Mandel, R., editor, *Guidebook of the 18th Biennial Meeting of the American Quaternary Association: Kansas Geological Survey Technical Series 21*, p. 3–B–1 – 3–B–12.

- Shackleton, N. J., and Opdyke, N. D., 1973, Oxygen isotope and Paleomagnetic Stratigraphy of Equatorial Pacific Core V28-238: Oxygen Isotope Temperatures and Ice Volumes on a  $10^3$  and  $10^6$  year scale: *Quaternary Research*, v. 3, p. 39–55, doi:10.1016/0033-5894(73)90052-5.
- Staiger, J. W., Gosse, J., Little, E. C., Utting, D. J., Finkel, R., Johnson, J. V., and Fastook, J., 2006, Glacial erosion and sediment dispersion from detrital cosmogenic nuclide analyses of till: *Quaternary Geochronology*, v. 1, p. 29–42, doi:10.1016/j.quageo.2006.06.009.
- Stone, J. O., 2000, Air pressure and cosmogenic isotope production: *Journal of Geophysical Research*, v. 105, p. 23,753–23,759, doi:10.1029/2000JB900181.
- 2004, Extraction of Al and Be from quartz for isotopic analysis. UW Cosmogenic Nuclide Lab Methods and Procedures. Online: <http://depts.washington.edu/cosmolab/chem.html>.
- York, D., 1966, Least-squares fitting of a straight line: *Canadian Journal of Physics*, v. 44, p. 1079–1086.